INVESTIGATION OF MECHANICAL PROPERTIES OF CERAMIC TILES DEVELOPED FROM SELECTED CLAY DEPOSITS IN UGANDA

BY

MUKWAYA GEORGE WILLIAM

A DISSERTATION SUBMITED TO THE DIRECTORATE OF RESEARCH AND GRADUATE TRAINING IN PARTIAL FULFILMENT OF THE REQUIREMENTS FOR THE AWARD OF THE DEGREE OF MASTER OF SCIENCE IN PHYSICS OF KYAMBOGO UNIVERSITY

OCTOBER 2023

DECLARATION

I, Mukwaya George William, do hereby declare that the work presented in this dissertation is my own and has not been presented to any University for an academic award.

Signed……

Date…….

APPROVAL

This is to certify that the work covered in this dissertation by Mukwaya George William was designed and carried out under our close supervision and is hereby dully approved for presentation to the Board of Graduate School and Senate of Kyambogo University.

Signed……...

SUPERVISOR ONE: Mr. Enjiku Ben DD

Department of Physics

Kyambogo University

Date…….…….

Signed…….

SUPERVISSOR TWO: Dr. Mukhokosi Emma Panzi

Department of Physics

Kyambogo University

Date……

DEDICATION

I dedicate this work to my lovely sister Ssekitoleko Catherine.

ACKNOWLEDGEMENT

I wish to express my special thanks to my father, Mr. Kasozi Duncan, for the love and financial support he extended to me during my primary, secondary and tertiary education. My late mother Ndagire Betty also deserves special thanks for the care and advice she gave me during my days in school.

My heart felt gratitude goes to my supervisors Mr. Enjiku Ben DD and Dr. Mukhokosi Emma Panzi for all the technical guidance and support they rendered to me during the course of carrying out the research and writing the final report. The time they spent reading and giving feedback to improve the dissertation was a constant encouragement for which I will forever appreciate their role.

My sincere thanks go to Mr. Ivan Fredrick Kalegga of Uganda Industrial Research Institute (UIRI) in the Department of Material Science for all the assistance he rendered to me during the formation and testing of the mechanical properties of the tile samples. Finally, I thank my relatives and friends especially my classmate Waiswa Tifus and Amooti Musinguzi for the spirit of team work they exhibited and I wish them success in all their endeavors.

TABLE OF CONTENTS

PAGE

LIST OF FIGURES

PAGE

PAGE

LIST OF TABLES

PAGE

ACRONYMS

MOR – Modulus of Rapture

C S – Compressive Strength

SEM – Scanning Electron Microscope

EDX – Energy Dispersive X-ray

XRF – X-ray Fluorescence

XRD – X-ray Diffraction

UIRI – Uganda Industrial Research Institute

EDS - Energy Dispersive Spectroscopy

ABSTRACT

In this study the characteristics of Buwambo kaolin, Lunya feldspar, Ntawo ball clay and Liddo beach sand were determined. The Modulus of Rapture (MOR) and Compressive Strength (CS) of the tiles produced using kaolin:feldspar of different composition ratios were determined. The composition ratios of kaolin:feldspar used were 4:3, 3:4, 5:9 and 2:5 by mass. On the other hand, a fixed composition ratio was used for ball clay:sand of 5:1 by mass (Ochen et.al 2012). The samples were fired at 1100 ^{0}C for 8 hours.

Using the scanning electron microscope (SEM), the Buwambo kaolin had a porous cellular structure of irregular-shaped particles of average size of 0.202 ± 0.131 µm. Liddo beach sand had porous particles with average particle size of 0.168 ± 0.198 µm, the Lunya feldspar had irregular confined particles with average particle size of 0.153 ± 0.105 µm and the Ntawo ball clay had fine grained uniform rounded particles of average size of 0.095 ± 0.055 µm. X-ray fluorescence (XRF) and Energy dispersive x-ray (EDX) spectroscopy were used to determine the elemental composition. The XRF on Liddo beach sand showed that it is mainly composed of 99.5 % SiO_2 with trace amounts of Al_2O_3 and Fe_2O_3 each 0.2 %. The EDX revealed that Buwambo kaolin mainly had 11.15 % Aluminium and 10.83 % Silicon. The Lunya feldspar mainly had 19.53 % Silicon and 5.46 % Sodium. The Ntawo ball clay mainly had 12.91 % silicon and 4.52 % aluminium. X-ray diffraction (XRD) on Liddo beach sand showed a broad reflection peak at 2θ = 22.86 ^{o} indicating its amorphous nature. The Lunya feldspar showed major peaks at 20.69, 26.40 and 29.52 ^{o} which are within the acceptable range of sodium feldspar. The Ntawo ball clay showed major peaks at 2θ = 20.82, 26.53 and 27.35 ^{o}. For Buwambo kaolin, the major peaks were located at 2θ = 12.29 and 27.40 ^{o}. The MOR and CS were significantly dependent on composition ratios at significant levels $\alpha = 0.01$ and $\alpha = 0.05$ and therefore the null hypotheses that the CS and MOR of the tiles produced are not affected by the composition ratios of the clay mixture rejected at the two levels of significance. The sample with the highest kaolin-feldspar ratio of 4:3 had the highest MOR of 30.84 ± 2.67 MPa at $\alpha = 0.01$ and 30.84 ± 1.60 MPa at α = 0.05. It also had the highest CS of 1.36 ± 0.06 MPa at $\alpha = 0.01$ and 1.36 ± 0.04 MPa at $\alpha = 0.05$. Similarly, the sample with the lowest kaolin-feldspar ratio of 2:5 had the least MOR of 18.58 ± 0.51 MPa at $\alpha = 0.01$ and 18.58 ± 0.31 MPa at $\alpha = 0.05$. It also had the least CS of 0.82 ± 0.03 MPa at $\alpha = 0.01$ and 0.82 ± 0.02 at $\alpha = 0.05$. Further investigation should be carried out using other clay deposits to find out how the variation in the amount of kaolin and feldspar in them would affect the CS and MOR of tile samples developed using these clays.

CHAPTER ONE: INTRODUCTION

1.1: Background of the Study

Construction has been an integral part of human activity since time immemorial to manage the harsh environmental and climatic conditions in which human beings find themselves. The construction sector has continued to develop by putting up different types of buildings and structures for industrial, institutional, commercial, residential and civil works. Over the years, much more resilient and long-lasting natural materials such as stone, wood, clay, concrete, bricks, metals, sand, lime bricks, concrete bricks, concrete blocks, non-clay bricks, plastics, and tiles were used. The initial adopted materials for construction in different parts of Uganda were the naturally occurring ones such as leaves, branches and animal hides. Later, more durable materials such as stones, timber and clay were developed. With the advancement in technology, bricks, metals, concrete, plastics and tiles were adopted to construct better structures. Concrete, bricks, metals, sand, lime bricks, concrete bricks, concrete blocks, plastics, and tiles are some of the most recent materials employed. All these construction materials are found to be resilient and durable.

Clay is one material that has been used for production of ceramics and other building materials. The word "ceramics" is derived from the Greek word "keramos," which means "burned things" or "products made by applying fire to materials." (Olupot P.W, 2010). Ceramic materials are clay products made of alumina and silica compounds joined by strong ionic and covalent bonds, giving them strength when in solid dry form (Grimshaw & Searle, 1971). Because of the strength of products made using ceramics, Egyptians used ceramic tiles to build the step pyramids in 2600 B.C. Ceramics were initially in the field of pottery which was used in the decoration of tombs. Fire bricks, insulators, sanitary ware, kitchen ware, resistors, magnetic memory systems, optical communication devices, and tiles were among the later applications for ceramics. For centuries, ceramic tiles have been used for decoration of both inside and outside buildings such as homes, places of worship, business structures to mention but a few. They are one of the oldest items used in decorative art because of their durability and beauty.

There are numerous tile types and names that can be used to describe the finished product, including: Ceramic, Porcelain, Mosaics, Encaustic, Cement and Natural Stone

tiles. Mosaics are made up of small pieces of tile laid on a sheet. When arranged and filled on a sheet, they give the impression of thousands of tiny tiles and are used in wet room showers. Encaustic tiles are prepared with coloured clays which run through the whole body. Porcelain tiles are produced using fine, heavy clays. Denser, finer clays are used to make ceramic tiles. However, due to their distinct beauty and durability, ceramic tiles are used and preferred today. Ceramic tiles are cheaper option to use and can be used on walls or floors of domestic houses as well as on commercial floors. Ceramic tiles do not easily attract dust, dirt, animal hair and thus they keep the structure free from any irritating dust particles that can cause problems for those who suffer from asthma and allergies. In addition, ceramic tiles do not need special maintenance since they can be maintained simply by sweeping any dust and dirt that collects on them. Tough stains, water and spills can be cleaned up by mopping the floor and they can also be cleaned using heavy-duty cleaner without any worries of causing damage. A properly kept ceramic tile can last between 10 and 20 years, making it one of the hardest and most lasting tiles available. Ceramic tile can only break under a big weight and therefore there is no need to worry about any cracks from heavy furniture. Unlike other types of flooring, Ceramic tile flooring is ideal for homes in warmer climates since it is heat resistant. They can also easily be installed. In case of a crack on the floor, one can easily fix the broken tile. Ceramic tiles have a high compressive strength and resistance to corrosion. On average, the cost of one square meter of ceramic tiles ranges from 35000 (9.6 Us dollars) to 80,000 Ugandan shillings (21.84 Us dollars) depending on the quality and size of the tiles. Because of all the above distinctive qualities of ceramic tiles, both in developed and developing nations, there is an increasing demand for installing tiles on the floors and walls of buildings.

Some research has been carried out on different clay deposits in Uganda involving the composition of the clays and the properties of the products of the clays. Appendix A summarizes some of the recent research carried out in Uganda involving Ugandan clays.

Although Olupot et. al (2010) characterized feldspar and quartz rich clay from Mutaka, Lunya and Liddo beach, they did not develop tiles using clays from these sites. Nyakairu et. al (2001) studied the effect of holding time on compressive strength of Ntawo ball clay but never developed tiles using clay from this site and never carried out

characterization of structural, surface morphology and thermal analysis of the clay. Kirabira et.al (2006) characterized the minerals from Mutaka, Mutundwe and Mukono clays but never developed tiles from the clays from these sites. Ochen et. al (2012) carried out limited studies on tiles using Mutaka Kaolin and feldspar rich clay, Ntawo ball clay in Mukono and Liddo beach sand from Wakiso focusing on the properties of Shrinkage, strength and water absorption of products from these clays.

Olupot e.t. al, (2010) characterized feldspar and quartz rich clays from Mutaka (Bushenyi), Lunya (Kayunga) and Liddo beach (Wakiso) in an effort to evaluate their potential as raw materials for making electrical porcelain insulators. The outcomes revealed that the feldspar-rich clay from Mutaka was completely microcline and acceptable for use with very little beneficiation, making it a good candidate for use in the production of electrical porcelain insulators. Nyakairu G. W. (2001) investigated how firing duration affected the compressive strength of slabs made from Mukono's Ntawo clay deposit. Results indicated that the compressive strength of ball clay beyond 800 ^{o}C did not need longer holding time since the compressive strength was not affected beyond this temperature. Kirabira et. al (2006) characterized raw mineral powders from Mutaka, Mutundwe and Ntawo clay deposits aiming at ascertaining their suitability for ceramic products development with emphasis of fire clay refractories. The bulk density obtained was 1938 kgm^{-3} (standard value between 1900 - 2000) and the cold crushing strength was 44 MPa (standard value must be greater than 22 MPa). These findings showed that the deposits recommended as viable and trustworthy sources of raw materials for the production of fire clay refractory bricks were Kaolin from Mutaka and Ball clay from Mukono.

Porcelain tiles were made by Ochen (2012) using kaolin and feldspar from Mutaka in Bushenyi, ball clay from Ntawo in Mukono, and sand from Liddo beach in Wakiso. According to the chemical analysis carried out by X-ray fluorescence method, results revealed 24.9 % alumina content in Mutaka Kaolin and 95.0 % Silica content in Liddo sand and 3.2 % Iron Oxide content in ball clay from Mukono. The tests carried out included Shrinkage, Strength and water absorption which were compared with South African National Standards. The tiles exhibited strength of 34 MPa, 0.0% water absorption and Shrinkage of 9% (wt). All these values were within South African National Standards for standard tiles (Ochen, 2012).

The properties of kaolin from Buwambo in Luwero, feldspar from Lunya, ball clay from Ntawo in Mukono and Sand from Liddo beach require further studies to characterize their crystal structure using XRD, mineralogical composition using EDX Spectroscopy and XRF spectroscopy, surface morphology using Scanning Electron Microscopy. It would also be of interest to investigate their mechanical properties to establish their suitability as raw materials for tile production.

1.2: Statement of the Problem

There has been a steady increase in the usage of tiles on almost every structure constructed in Uganda. There exists plenty of clay deposits in different parts of Uganda that can be used to satisfy the construction industry demand for tile in the country but what is so far lacking is obtaining the dependable knowledge about the suitability of the local clays in terms of the composition, structure and potential or suitability of these various clays to produce ceramic tiles.

1.3: Purpose of the Study

This study was to develop tiles using clays from selected clay deposits in Uganda and investigate the surface morphology, crystallographic structure and mineralogical composition of raw materials used and determine their mechanical properties.

1.4: Objectives of the Study

i. To determine the surface morphology, crystallographic structure and mineralogical composition of the clay materials used in the study.
ii. Investigate the Compressive Strength of the tiles produced using different mixture ratios of the four clay types.
iii. Investigate the Modulus of Rapture of the tiles produced using different mixture ratios of the four clay types.

1.5: Hypothesis to be Tested

Following objectives (ii) and (iii), the null hypotheses below were tested;

HO_1: The Compressive Strength of the tiles produced is not affected by the composition ratios of the clay mixture.

HO_2: The modulus of rapture of the tiles produced is not affected by the composition ratios of the clay mixture.

1.6: Scope of the Study

The study was limited to the use of ball clay from Ntawo in Mukono district, Wakiso sand in Liddo beach Entebbe, Buwambo kaolin clay from Luwero district and feldspar clay in Lunya village in Kayunga all located in Uganda.

Four different ratios of ball clay : kaolin : feldspar : sand were prepared as A (5:8:6:1), B (5:6:8:1), C (5:5:9:1) and D (5:4:10:1). The values of kaolin and feldspar were varied while keeping ball clay and sand constant. These ratios were used to make four different samples of the tiles. The compressive strength and modulus of rapture of the tiles were determined using universal testing equipments located at Uganda Industrial Research Institute (UIRI).

1.7: Significance of the Study

Production of ceramic tiles from different composition ratios of ball clay, kaolin feldspar and sand will provide information to manufacturers on the most appropriate mixtures in order to optimize the CS strength and MOR of the tiles.

The results of this study reaffirm the sources of raw materials required for manufacturers of ceramic tiles.

The ratios of the clay used are to provide useful information for companies for suitable ratios of clays to produce acceptable tiles.

CHAPTER TWO: REVIEW OF RELATED LITERATURE

2.1: Introduction

This chapter is structured in six subsections. The first section discusses how clay is formed leading to the different types of clay. This is followed by clay composition and mineralogy. The clay types used in tile formation are also discussed. Furthermore, the properties of clay used in tile production, history of tiles and the mechanical properties of ceramic tiles are discussed. This is finally followed by determination of characteristics of the raw materials using Energy Dispersive X-ray Spectrometry, X-ray Diffractometry, X-ray Fluorescence and Scanning Electron Microscopy.

2.2: Formation of Clay and their Major Classes

Clay is a natural material that is formed by weathering of rocks and it is always composed of a mixture of minerals. It is a material with a diameter less than 0.005 mm and contains fine grained particles of hydrous alumina silicates which gains plasticity at given water content (Grimshaw & Searle, 1971). Clay has the ability to interact with water. One of the main characteristic of clay is its highly hygroscopic behavior. The water molecules retained in the crystal structure of clay makes it plastic. The flexibility of clay is a feature that results from the presence of water molecules in its crystal structure. This property of plasticity allows clay to be molded into any shape when mixed with water. Clay may be formed into any shape, which it can then hold after drying and hardening, though heat can cause it to lose its fluidity. The two types of clays are transported clays, commonly referred to as sedimentary clay, and residual clay. Surface weathering produces clay in three different ways, resulting in the formation of the residual clays. These processes include the chemical breakdown of silica and alumina-containing rocks like granite, the solution of clay-impurity-containing rocks like limestone that are deposited as clay, and the disintegration and solution of clay shale. The transported clay is clay removed from the place of origin by erosion which is deposited in another distant position. Different clay deposits have clays with different characteristics (Singer & Singer, 1963) and the samples of clay from the same deposit may differ in their mineralogical content. The residual clay and transported clay contain clay minerals.

2.3: Clay Composition and Minerals

Clay is composed of minerals. The earth's typical clay minerals are those that are found close to the planetary surface environment. They contain various concentrations of ions, including cations, magnesium, metals, iron, alkali, and alkaline earth metals. They are useful components of soil and are formed by digenetic and hydrothermal alteration of rocks in presence of water (Abdulabbas, 2022). Mudstone, shadow, and siltstone are examples of fine-grained sedimentary rocks that commonly contain clay particles. They have the ability to act as chemical sponges because they can hold water and dissolved plant nutrients that are eroded from other minerals due to the presence of an unbalanced electrical charge on their surface (Kerr, 1952).

Hydrous aluminum phyllosilicate, also known as hydrous alumino silicate, is the name given to the majority of clay minerals. This is because the production of clay minerals requires water. Chemical weathering of rocks causes the formation of clay minerals. The basic minerals present in the earth's crust and clay minerals share a similar chemical and structural makeup. Primary and secondary minerals make up the group of minerals that make up clay. Primary clay minerals include quartz, mica, kaolinite and feldspar. They are the most resistant and they remain in the soils. The primary minerals which are less resistant are susceptible to break down by weathering and include pyroxenes and amphiboles. On break down, they form secondary minerals. The secondary minerals are phyllosilicates because they show a platy structure with irregular edges and possess an extended tetrahedral silicate (SiO_4) as an important basic structural unit. Secondary minerals arise as a result of either neoformation— the formation of a more stable structure through the precipitation or recrystallization of dissolved primary mineral elements —or adjusting the primary mineral structure (Lal, 2006).

Clay minerals are often made up of ultra-fine particles, with size less than 2 μm. Clay minerals include kaolinite, smectite, chlorite, feldspar and micas. They are the main building blocks of clay's raw materials and form when there is water present. They have silica, alumina, variable amounts of inorganic ions like Mg^{2+}, Na^{+}, Ca^{2+} and water thus known as hydrous phyllosilicate. Tetrahedral (SiO_4) and octahedral (Al_2O_3) sheets are two-dimensional sheets found in clay minerals. The mother of clay is the mineral group called feldspar. The composition of the feldspar is altered by the hydrolysis process during weathering. As a result, clay minerals are created, such as kaolinite, the primary ingredient in kaolin clays, and smectite, the primary ingredient in bentonite clays. Even in

the presence of minor concentrations of metal oxides (Al2O3, MgO, etc.), quartz (SiO2), and organic matter, clay can combine with one or more clay minerals. (Kumari & Mohan, 2021). The clay's shape, particle size, and water content all contribute to its fluidity. Clay becomes stiff, hard, coherent and non-plastic after firing and drying. The clay's flexibility and ability to harden are significantly influenced by the chemical composition of the mineral that makes up the clay. The composition of clay minerals is determined by the chemical compounds that are present there, the way the atoms and ions are arranged, and the forces that hold the atoms together. Most clay minerals are complex silicates of various ions, including iron, aluminum, and magnesium. The silicon-oxygen tetrahedron and the aluminum or magnesium octahedron are the two different types of basic crystalline units found in clay minerals. The aluminum or magnesium octahedron is made up of six hydroxyl units surrounding the main dominating atoms of aluminum or magnesium, which together form gibbsite for aluminum and brucite sheet for magnesium. Four oxygen atoms surround silicon in the silicon-oxygen tetrahedron, which together make up the silica sheet.

The chemical composition of kaolin is thus made of $Al_2O_3Si_2O_5(OH)_4$ compound implying sheets of $n(Si_2O_5)^{2-}$ link to $(Al_2(OH)_4)^{2+}$ units, where n is a whole number. These sheets are linked by hydrogen bonds which are weaker compared to ionic and covalent bonds. All kaolin minerals are crystalline and they have the same basic structure. The difference between them being the way these pairs of layers are stacked on top of one another to form a crystal. Due to its relatively coarse grain structure, low dry strength, and low firing shrinkage, kaolin gives plasticity to the clay mixture. Pure kaolin is the best choice of clay to be used for samples that are to be white and clean. Kaolin is frequently the only type of raw clay used in ceramic tile manufacturing; however, it has a lower plasticity than other raw clay varieties. If kaolin is used alone, enough plasticity may not be achieved more so for non-casting plastic forming bodies. Plasticizers like ball clays and bentonites are often added. Bentonites, highly plastic kaolins, and white burning ball clays can all be used if translucency and whiteness are required. The particle size of kaolinite mineral is significantly greater than that of ball clay and bentonite materials. They can offer a good cross section of ultimate particle size if they are blended in bodies, which promotes improved working and drying qualities. Furthermore, kaolin is more permeable to passage of water because of its larger particle size. The larger-sized kaolin has faster drying and casting rates across all body types. The primary source of

alumina is kaolin from the Mutaka deposit, and the primary plasticizer and binder is ball clay from Mukono (Kirabira, Wijk, Jonsson, & Byaruhanga, 2006). Tetrahedral and octahedral layers are present in kaolinite clay minerals at a ratio of 1:1.

Additional forms of clay minerals are expanding and non-expanding minerals. Vermiculite and clay minerals from the Smectite group are examples of expanding clay minerals. These expand when wet. Smectite are based on trioctahedral (Saponites) or dioctahedral (Montmorillonite) structure. The general structural formula of smectite clay is $(Na, Ca)_{0.33}(AL, Mg)_2Si_4O_{10}(OH)2.(H_2O)_n$ (Kumari & Mohan, 2021). The exchangeable ions in the smectite structure are responsible for the different unique properties such as high adsorption capacity, high cation exchange capacity (quantity of cations needed to balance the charge deficiency) and high surface area of the clay. Tetrahedral and octahedral layers in the ratio of 2:1 are used to classify the smectite clay mineral.

Bentonite clay, also known as sedimentary clay, is a member of the Smectite family. It is an impure form of aluminium phyllosilicate clay made by di-vitrifying volcanic ash and weathering the parent rock chemically or mechanically in the presence of water. It contains 98% Montmorillonite. It has a unique property of water retaining. Different types of bentonites exist based on the dominant metallic elements such as sodium (Na), potassium (K), Aluminium (Al) and calcium (Ca). There are three major types of bentonites for industrial purposes and these are; calcium, potassium and sodium bentonites. Calcium bentonites are good adsorbent for ions, lipids and oils and can be transformed to sodium bentonite by ion exchange procedure. Drilling mud for gas and oil wells contains sodium bentonites. Additionally, they are utilized in boreholes for geotechnical and environmental research (Odom, Fowden, Barrer, & Tinker, 1984).

Layer expansion is prevented by the charge deficiency of non-expanding clay minerals, which are balanced by K-ions in the interlayer space and serve as a bridge between the layers. They cease to expand as a result. They have a chemical formula of $(K,H_3O)(Al,Mg,Fe)_2(Si,Al)_4O_{10}[(OH)_2,(H_2O$Muscovite, biotite, and the clay mineral mica (illite) are a few examples of non-expanding clay minerals. Muscovite and feldspar, which are present in soil, sedimentary rocks, and low-grade metamorphic rocks, combine to form illite. The presence of 20% aluminum atoms in illite causes the tetrahedral sheet

to have a greater negative charge. Illite has a smaller cation-exchange capacity than smectite but higher than kaolinite.

Chlorite is another type of non-expanding clay mineral which belongs to silicate group (iron-magnesium silicates). Chlorite crystals such as vermiculites clay minerals are made of 2:1 tetrahedral and octahedral layers. They alternate with tri-octahedral sheets (brucite) that are dominated by magnesium, resulting in a 2:1:1 layer ratio. Magnesium ions occupy every octahedral position in the mineral chlorite, and while their negative charge is lower than that of smectite and vermiculites, it is nearly equal to that of fine-grained mica. Since there is no adsorption of water between the layers, chlorite does not expand. Chlorites have a chemical formula of $Al_4.33(Si_3Al)O10(OH)_8$ (Grim & Kodama, 2021). Chlorite clay mineral is categorized based on the presence of tetrahedral, octahedral and octahedral layers in the ratio of 2:1:1. Several of the abundant ceramic refractory minerals found throughout the nation include: silica raw materials (SiO_2), fireclay, alumina raw materials (Al_2O_3) (kyanite, andalusite, sillimanite and corundum), magnesia raw materials (MgO) (magnesite) and forsterite raw materials (Fe_2O_3) (talc, pyrophyllite, serpentine asbestos). Oil absorbents, iron casting, animal feeds, pottery, china, pharmaceuticals, drilling fluids, waste water treatment, and food preparation are just a few of the many applications for clay minerals, which are categorized based on variations in their chemical composition and atomic structure.

The clay type called China clay is a residual clay and is composed of clay with a high proportion of kaolinite mineral mixed with silica, feldspar and mica (Ryan, 1978). China clay is used in the production of white decorative ware and in refractory because of its low impurity content. In the manufacture of ceramic tiles, kaolin is employed as the major source of alumina because the higher the alumina contents in the mixture the greater the strength of the ware formed (Peter Wilberforce Olupot, Jonsson, & Byaruhanga, 2006).

Kaolin clay has poor plasticity that makes it difficult to be shaped into other shapes therefore it is not used alone when developing ceramic tiles. When kaolin is used alone, it becomes difficult for it to mature into a hard and dense body needed in firing. Kaolin has to be added to other minerals like feldspar and ball clay to improve on its plasticity and also reduce the firing temperatures in order to produce hard and dense ceramic tiles

(Kirabira et al., 2006). Quartz is the major impurity in kaolin and ball clay and this can be removed by sieving. The clay particles tighten into a dense structure at a temperature of about 1300 ^{o}C (Islam, 2002).

The Feldspar clay is used in ceramics as fine powders and it acts as a flux by forming a glassy phase on the ceramic body. This improves on vitrification and translucency of the ceramic body (P. W. Olupot, 2010). Both potassium and sodium feldspar melt at temperatures between 1100 ^{o}C to 1200 ^{o}C. The glassy phase formed as a result of melting of feldspar fill the pores created hence increase in strength and decrease of water absorption of the ceramic body (Abadir, Sallam, & Bakr, 2002). Sand is purely silica (SiO_2) in nature. Sand is used in the manufacture of ceramic tiles to avoid warping. Sand maintains the shape of the fired body by reducing shrinkage. This is because sand has a high melting point therefore at high temperature it cements the gaps created hence maintaining shape (Grimshaw & Searle, 1971). Sand must be used as a fine powder whose particle size ranges between 0.05 and 2 mm. This is because the expansion of crystals in a matrix due to heating, leads to stress that may give rise to cracking (Kingery, Bowen, & Uhlmann, 1976). The stress in the grains can be reduced if the grain size is reduced; therefore properties of stoneware are improved if fine grains are used instead of coarse material(Stathis, Ekonomakou, Stournaras, & Ftikos, 2004).

2.4: Clay Types in Tile Production

Earthen ware, stone ware and ceramic tiles are produced when different clay types with varying mineralogical composition and firing conditions are used. These are generally called ceramic materials. The ceramic tile body is made up of several typologies of raw materials basing on the characteristics of the product required. The sample composition and treatment conditions determines the transformation which contains the raw materials and this describes the final features and field of application of the final product (Elakhame, Ifebhor, & Asotah, 2016). The types of clay recognized contain mainly silicate and alumina which are crystalline and amorphous in nature. The size of the grain enables the materials to be classified into coarse-crystalline, in which the grains are readily visible to the unaided eyes, fine or microcrystalline in which the grains are much finer such that they require a strong microscope to identify their structure. Though many ceramic materials especially plastic clay appears to be amorphous under a microscope, the use of x-rays and an electronic microscope shows that they are crystalline in nature

(Grimshaw & Searle, 1971). The various raw materials needed for the production of ceramic tile body include: Black clay, stone dust (granite powder), feldspar, lime stone, quartz, Talc, red clay, white clay, kaolin and water. Ceramic tiles are commonly made from clays although recent technological advancement has resulted into plastic, rubber or glass tiles. Ceramic floor tiles are made from clay mixed with other ingredients like feldspar and sand. During the formation of ceramic tiles, two categories of clay are used. These are; kaolin and ball clay and each has an important purpose in the manufacture of the ceramic object and in the properties of the finished ceramic product (P. W. Olupot, 2010).

The word kaolin and kaolinite originated from china where Chinese used white clay for production of ceramic materials. Kaolin is sometimes called china clay. Kaolin is soft, white and can easily be dispersed in water. It is plastic when moist and it hardens when dry. These are the main features which can be used to distinguish kaolin from other minerals. Kaolin is widely employed in the manufacture of ceramic tiles, paper industry as a coating/filler material, paint industry, ink, medicine, cosmetics etc. Kaolin is usually formed from strong weathering of rocks mostly acidic rocks like granite. Kaolinite is the main mineral which is contained in kaolin with a chemical formula of $AL_2O_3.2SiO_2.2H_2O$. Pure kaolin contains 46 % silicate, 40 % Alumina and 14 % water. However, it is not easy to find pure kaolin because of impurities like Fe_2O_3, Lime (CaO), Titan (TiO_2) and Potassium (K_2O). According to figure 2.1, the kaolinite mineral has a 1:1 dioctahedral layer structure, with each layer made up of a single silica tetrahedral sheet and a single alumina octahedral sheet.

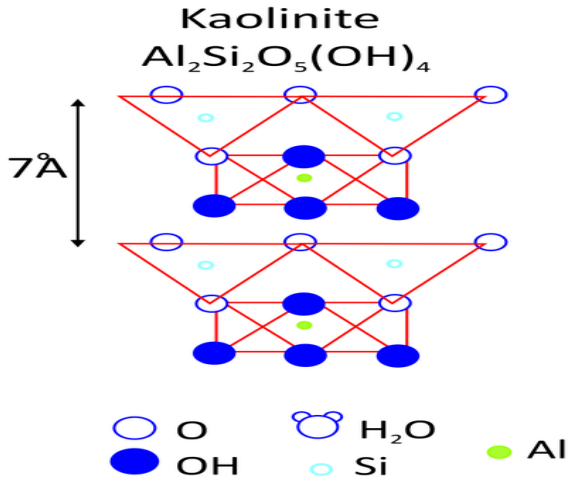

Figure 2.1: Chemical **s**tructure of Kaolin (Bauluz, 2015).

Different purity levels of kaolin are available for purchase, and the more pure the kaolin, the more expensive it is. In this study, the characteristics of impure kaolin were examined using XRD and the results compared with pure kaolin characteristics based on literature.

Ball clay derived its name from the ancient times when clay was mined by hand. The clay was rounded into balls during transportation. It is sedimentary in origin where kaolin flew through streams from upland areas and mixed with other clay minerals, vegetation gravel, sand and settled in low-lying basins thus forming closures of ball clay. It is a fine - textured and plastic clay which is mainly used in the production of ceramic products such as sanitary ware, tableware, electrical porcelain insulators and tiles. Ball clays are kaolinitic clays made up of 20 – 80 % kaolinite, 10 – 25 % mica, 6 – 65 % quartz and organic matter. Therefore, ball clay has variable compositions and consists of a mixture of three minerals i.e. kaolinite, mica and quartz in which kaolinite is the key mineral. Table 2.1 shows the chemical composition of each mineral in ball clay.

Table 2.1: Major minerals in ball clay

Mineral	Components	Chemical Formula
Kaolinite		$Al_2O_3.2SiO_2.2H_2O$ (Bergaya & Lagaly, 2006)
Mica	Muscovite (a hydrated silicate of aluminium and potassium)	$KAl_2(AlSi_3O_{10})(F,OH)_2$ (Bergaya & Lagaly, 2006)
	Phlogopite (potassium magnesium aluminium silicate hydroxide)	$K_2Mg_6(Si_6Al_2O_{20})(OH)_4$ (Bergaya & Lagaly, 2006)
Quartz	Silicon dioxide (silica)	SiO_2 (Bergaya & Lagaly, 2006)

The respective structures of the minerals in ball clay are shown in figure 2.2.

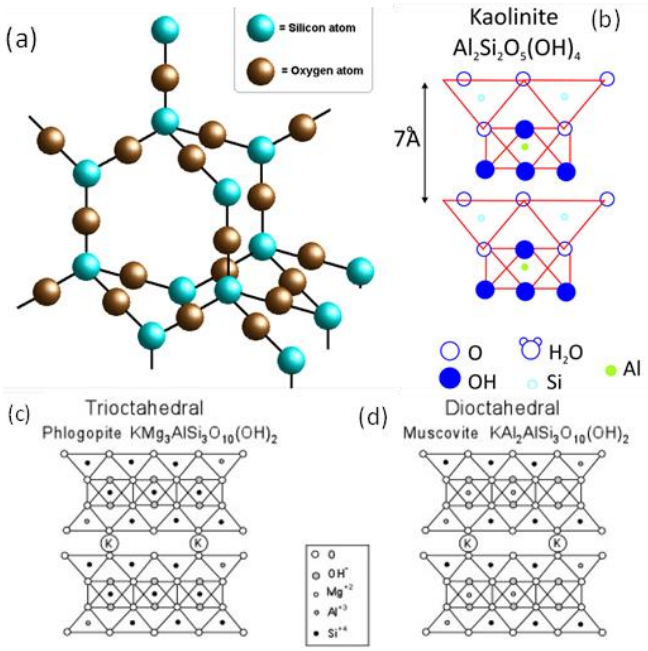

Figure 2.2: Chemical structures of minerals in Ball Clay (Bauluz, 2015; Nelson, 2015).

The color of moist ball clay ranges from grey to brown and white for kaolin. This variation in ball clay is due to presence of iron and other impurities. Kaolin mineral is a combination of two layers: The first is the silica layer made of silicon and oxygen atoms. Secondly is the gibbsite layer made of aluminum atom and the hydroxyl group (Young, 2019). Because it increases the body's workability in the plastic state, ball clay is used to make ceramic tiles. (Singer, 2013). Because ball clay contains significant amounts of iron oxide and titania, which somewhat reduce the whiteness of the fired bodies and subsequently decrease the translucency of the vitreous ware, the amount of ball clay in the white ware must be kept under control. If whiteness is desired, a clay body may contain no more than 15% ball clay (Powell, 1996).

Feldspar is a term derived from Germany which is a short form of the word field spar since some specimens were initially found in fields. The word spar is a general term which means non-metallic minerals with glassy (vitreous) luster. The earth's crust is majorly composed of feldspar rock forming mineral up to about 60 %. They are alumino-silicate minerals, mostly found in igneous rocks, made up of varying amounts of sodium, potassium, or calcium. The chemical name of the feldspar is derived from the form of the alkali metal which is found in the molecule and the most common ones are Potassium aluminium silicates **(**$KAlSi_3O_8$), sodium aluminium silicates ($NaAlSi_3O_8$) and calcium aluminium silicates ($CaAl_2Si_2O_8$). Potash and soda feldspars crystallize from magma of

igneous, metamorphic and sedimentary rocks. They are the most significant members of the feldspar family from a commercial standpoint. They are widely used in industries that manufacture glass, ceramics, rubber, paint, plastic and welding electrode as filling material. They are primarily used as a fluxing material in the glass industry to speed up melting and reduce fuel consumption. The aluminium content aids in the resistance of thermal shock and improve mechanical properties, thermal durability and prevent devitrification. Potash feldspar makes the product stronger, transparent and gives it higher viscosity compared to soda feldspar. During the manufacture of ceramic tiles, Sodium-potassium feldspars are mainly used. The silicon ions in any structure form a three-dimensional network in the mineral that is connected by shared oxygen ions. The structure of Sodium aluminium silicates feldspar ($NaAlSi_3O_8$) is as shown in figure 2.3.

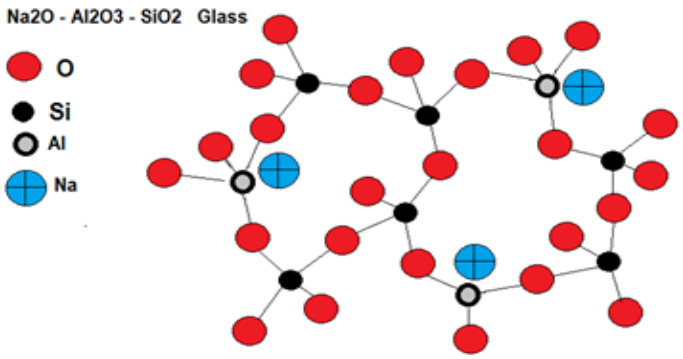

Figure 2.3: Chemical structure of Sodium Aluminum silicates feldspar ($NaAlSi_3O_8$), (Kumari & Mohan, 2021).

The structure of Potassium Aluminum Silicates **(**$KAlSi_3O_8$) feldspar is as shown in the figure 2.4.

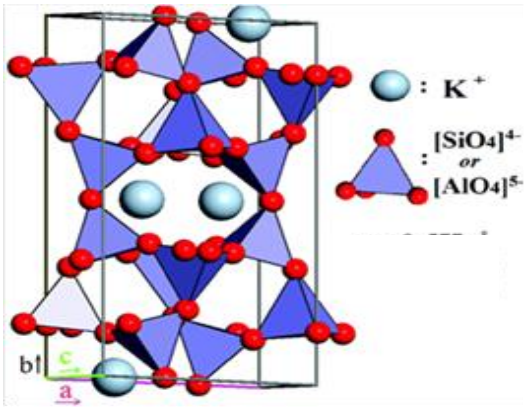

Figure 2.4: Chemical structure of Potassium Aluminum Silicates **(**$KAlSi_3O_8$) feldspar, microcline (Zhang et al., 2018).

Sand is a solid material made up of finely divided mineral particles formed when rocks break down from weathering and erosion. Its composition varies depending on the rock type; however, the most common constituent of sand is silicon dioxide (SiO_2), commonly known as silica usually in the form of quartz. Silica may be classified as crystalline or amorphous (non- crystalline). When the silicon and the oxygen atoms are arranged in a fixed geometric pattern, they form crystalline silica while amorphous silica is one where there is no spatial ordering of the silicon and oxygen atoms. The chemical composition of sand is the compound silicon dioxide (SiO_2) whose crystalline and amorphous structures are as shown in figure 2.5

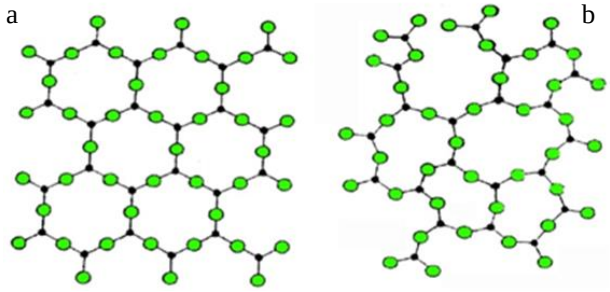

Figure 2.5: (a) Crystalline structure of Silica (b) Amorphous structure of Silica (Takada, Richet, Catlow, & Price, 2004).

Sand is mainly used during the construction of roads, buildings and in the manufacture of construction materials such as bricks, pipes, concrete blocks and ceramic tiles. The tiles can be glazed and this makes them more slippery. Ceramic tiles can be used either on walls, floors, or roofs. Rubber floor tiles are more useful in areas which require protection from easily breakable floor. They are commonly used in; flooring of workshops, garages and gyms. Plastic floor tiles are the most recent innovation and these are used in areas vulnerable to contamination by oils, grease and chemicals. They are commonly used in chemical factories, shops and even school laboratories.

2.5: Preparation of Clay in Production of Tiles

Ceramics are inorganic, non- metallic minerals formed between aluminum and oxygen, calcium and oxygen, silicon and nitrogen (Olupot P.W, 2010). Ceramic materials are made up of mainly covalent and ionic bonds making them strong in compression but weak in tension or shear hence brittleness. Most of the raw materials used by refractory manufactures are naturally occurring. There are different ways in which refractories are prepared so as to lower the fluxes and unwanted oxides. Refractory materials are based

on six main oxides: Silica (SiO_2), Alumina (Al_2O_3), Magnesia (MgO), Calcia (CaO), Cromia (Cr_2O_3), and Zirconia (ZrO_2). Refractories based on Carbon and combination of carbon with other elements also exist. e.g. Silicon Carbide (SiC). It is used in applications that need extreme resistance to heat such as bricks and ceramic tiles. The ceramic tile body is made up of several typologies of raw materials basing on the characteristics of the product required. The sample composition and the conditions of treatment determines the transformation which contains the raw materials and this describes the final features and field of application of the final product (Elakhame et al., 2016). The various raw materials required to make ceramic tile bodies include: Black clay, stone dust (granite powder), feldspar, lime stone, quartz, Talc, red clay, white clay, kaolin and water.

The basic principles of crystal structures and bonding give a better understanding of the different strengths and characteristics between metallic and non- metallic materials (Grimshaw & Searle, 1971). Ceramics are inorganic, non- metallic minerals formed between aluminum and oxygen, calcium and oxygen, silicon and nitrogen (Olupot P.W, and Byaruhanga, 2008). The type of bonding between atoms and the way atoms are packed together in ceramics primarily affects the mechanical, magnetic, chemical, electrical and optical properties of ceramics. The main types of bonds present in a crystal lattice are covalent and ionic bonds in which electrons are shared between adjacent bonds. Other types of bonds include metallic, hydrogen and van der walls bonds which are weaker. The types of bonds mainly present in ceramic materials are covalent and ionic bonds (Kingery W.D et al, 1976). The ionic character is given by difference in electro-negativity between cations and anions while the covalent nature is given by sharing of valence electrons (Grimshaw & Searle, 1971). Materials with covalent and ionic bonds are stronger, rigid at room temperature, hard and rapture after a small displacement. This is because of the covalent bonds present (Smallman & Ngan, 2011). When a crystal containing ionic or covalent bond is subjected to compression, the ionic components or atoms are forced close to each other hence strengthening the bonds. If a similar material is subjected to tensional or shear force, the atoms are pulled from their equilibrium position hence weakening the bond resulting into cracks or breakage. Ceramic materials are made up of mainly covalent and ionic bonds making them strong in compression but weak in tension or shear hence brittleness. Similarities and differences between clay minerals depend very much on their crystal structure.

Beginning around 4000 BC, ceramic tiles were first used in Egypt. Romans, Assyrians and Babylonians also made ceramic tiles which were produced in form of different geometric designs including plants, flowers, birds and people. The decorative ceramic tiles became popular during the Islamic period from the 12th century which were used in the decoration of the inside and outside of buildings such as mosques. The Moraq method was employed to create the ceramic tiles, which involved cutting single-color ceramic tiles into tiny shapes and connecting them by pouring plaster between them to create panels. The panels after drying and hardening were then put together on the walls of structures. In Europe, beautiful ceramic tiles grew in popularity during the middle Ages. They originated in Spain during the Moorish era and then extended to the surrounding nations and the rest of Europe. The wealthy, monarchs, churches, and other ecclesiastical institutions were the only ones who could afford these pricey ornamental tiles. The use of ceramic tiles, which were created of various colors and forms and baked together to create powerful patterns that were ingrained in the tile making the design robust and not easily broken, gained popularity throughout Europe.

Painted tiles were employed in churches and other places of worship during the European Middle Ages. To help the illiterate people who couldn't read and understand the biblical stories, scenes from the Bible were painted on these tiles. Additionally, Christian writings were written in Letter Tiles on church floors. Up to 1600’s and beyond, ceramic tiles were still in demand. The Delftware tiles, known for their cobalt blue and white hues, were created in Holland in the 17th and 18th centuries. These were well-liked both in the American colonies and in Europe. The colonists used them to decorate their homes' walls as well as the regions surrounding their fireplaces.

Instead of making ceramic tiles by hand, new manufacturing techniques were introduced as a result of the industrial revolution. This led to mass production of ceramic tiles in developed countries like Britain which started producing the tiles at more affordable prices for middle class people. However, ceramic tiles that were painted and manufactured by hand remained popular among those who could afford them. The mass productions which were cheaper helped the ordinary people to use them. Ceramic tiles were seen as a more hygienic type of flooring for structures. Early in the 20th century, ceramic tiles remained popular, notably the subway tiles that were created and first used on the walls of New York City subway stations. These white tiles were installed in

bathrooms and kitchens. In the twenty-first century, decorative ceramic tiles are still widely utilized to create eye-catching displays both inside and outside of homes, offices, and institutions of all types. Modern ceramic tiles can be used on walls, bathrooms, kitchens, and paths and come in a variety of hues.

According to the Ceramic World Review's annual survey of ceramic tile production, consumption, exports, and imports, the world's ceramic tile production reached 5,904 million square meters in 2002, an increase of 5.5 % from numbers from the previous year. The Middle East, particularly Iran, Brazil, and mostly Asian nations like China and India were responsible for this surge in production. Due to wide availability of clay deposits and improving technologies in the different parts of the world, the production of ceramic tiles in developed countries has increased and consequently the exports of ceramic tiles within the developed countries has decreased. This is not the case to developing countries because their exports to developing countries have continued to increase. However, the exports of Italy, one of the leading manufacturers of ceramic tiles continued to fall because developing countries had started adopting the new technologies and manufacturing their own ceramic tiles. China developed independent technological development which created competition to Italian ceramic tile manufactures. Ceramic tile production by developing countries continued to increase due to the demand of these tiles in the developing countries. For instance, manufacturing in Spain climbed by 2 %, in North America by 13.5 % to 219 million square meters, and in Brazil by 5 % to 35 million square meters. The ceramic tile production in Asia increased by 538 million square meters while Africa recorded the largest percentage increase from 115 million square meters to 192 million square meters (Ceramic world. Web 2021). This increase indicates rising need in the production and usage of ceramic tiles as indicated in the table 2.1

Table 2.2: Global Manufacturing output of Ceramic Tiles (Ceramic world. Web 2021).

Countries	Production output Square meters	% of World Production
European Union	1,449	24.5
Spain	651	11.0
Italy	606	10.3
Other Europe (Turkey included)	344	5.8
North America (Mexico included)	219	3.7
Central (South America)	597	10.1
Brazil	508	8.6
Asia	3098	52.5
China	2,100	35.6
Africa	192	3.3
Oceania	5	0.1
Total	5904	100

By 2020, China was the leading ceramic tile manufacturer worldwide manufacturing 8.47 billion square meters, followed by India with 1.32 billion square meters followed by Brazil manufacturing 840 million square meters. Vietnam is known to be producing 534 million square meters, Spain making 488 million square meters, Iran making 449 million square meters, Turkey making 370 million square meters, Italy making 344 million square meters, Indonesia making 304 million square meters and Egypt manufacturing 285 million square meters. Africa produced 918 million square meters of ceramic tiles by 2020, an increase from the 310 million square meters produced in 2008. By 2020, 1,124 million square feet of ceramic tiles had been consumed in Africa. The building and construction industry is the major industry that is responsible for increased demand for ceramic tiles in Uganda. In Uganda, the demand for ceramic tiles is increasing quickly, at a rate of about 3 % annually. This is a result of the nation's industrial sector's explosive growth. The ceramic tile market for both external and interior use is growing both in rural

and urban areas. Recently, the ceramic tile market increase is estimated from 3.8 % in 2009 to 9.1 %.

2.6: Mechanical Properties of Ceramic Tiles

A material's mechanical property is a gauge of how well it can withstand an external mechanical force. These include compressive strength, modulus of rapture, bulk density, ductility, hardness, impact resistance and fracture toughness. The different mechanical data has been published about ceramic tiles that determine the strength of the tiles which includes: fracture toughness, elastic moduli, 3-point and 4-point modulus of rupture, Poisson coefficient, impact strength, critical defect size, creep, micro-hardness, Weibull modulus and wear rates (Dondi, 2007). Another important mechanical strength measurement is CS.

It is the capacity of the tile to withstand loads tending to reduce its size. The CS of a ceramic tile makes it to resist being pushed together. The strength of ceramic materials is associated with its ability to withstand pressure being applied to it without rupturing. Strong ceramic materials have a capacity to be stretched or compressed without fracture. Shape, size and distribution of the particles have a direct impact on the hardness and strength. The magnitude of CS of a ceramic tile is dependent on the purpose which the tile is being made for. For the case of floor tiles the standard compressive strength ranges from 700 N and above. Most of the tiles on market can withstand forces that range between 800 N to 1100 N.

The MOR or transverse rapture strength is another important property of a ceramic tile which is the stress in a ceramic tile just before it yields in a flexure test. The breaking force is the force required to cause a ceramic tile to break and it is determined using the pressure gauge. The breaking strength is the force found by multiplying the breaking load by the width of the ceramic tile. The MOR is obtained by dividing the calculated breaking strength by the square of the minimum thickness along a broken tile edge. The MOR is used to determine the strength of ceramic samples using three-point loading test. The three-point loading test method involves two cylindrical rods made of metals in contact with the test specimen with length, l, projecting from either side of the specimen, one rod is slightly pivoted and the other rod rotatable (ISO 10545-4, 1994). The central cylindrical rod of the same diameter is used for transmission of the load force, F. Ceramic

tiles can be manufactured by either extrusion or pressing method. The recognized standard MOR of ceramic floor tiles should be above 27 MPa (Luz & Ribeiro, 2007).

In the refractory industry, ceramics are used to make fire bricks and insulators. This is because of their durability at high temperatures (Smallman & Ngan, 2011). A ceramic material that maintains its shape and chemical identity when exposed to high temperatures is called a refractory. Ceramic tiles are attractive, easy to clean, durable and replaceable in case of any damage. The type of traffic caused by pedestrians, type of shoe heel or sole type (rubber or metal) must be considered before using a specific ceramic tile group. The amount and frequency of the traffic should also be considered in choosing tiles for floor use. Class one (A1 or B1) ceramic tiles are suitable for low traffic domestic areas such as bathrooms and toilets. Class two (A2 or B2) are suitable in domestic areas where normal foot wear is worn like in the living rooms and bedrooms. Class three (A3 or B3) tiles are suitable for entire domestic areas such as kitchens, bathrooms, living rooms and bedrooms and also commercial areas subjected to light traffic. Class four tiles (A4 or B4) are suitable for use in high traffic areas which include hospitals, public buildings, shopping malls, schools and restaurants. The size and shape of individual clay particles have an important influence on ceramic properties. The particle sizes are very small, about stem ranging down to colloidal dimensions. It is this characteristic that is largely responsible for their plasticity when mixed with water. Ceramic tiles are the most popular types of tiles used in flooring and covering walls of homes, offices, and public buildings. Because of the different applications of ceramic tiles, the mechanical properties of ceramic tiles are considered to determine the stress the tiles can withstand.

2.7: Mineralogical Composition, Crystal Structure and Surface Morphology of Materials.

The chemical and mechanical structure and composition of soils and rocks are altered by decomposition, which is brought on by atmospheric factors. The rocks are degraded mechanically by splitting into smaller pieces while they are degraded chemically by changing in their mineral composition through processes such as carbonation, oxidation and reduction. The industrial behaviors of soils/rocks are determined by their geological history (Baynes, Fookes, Kennedy, & Environment, 2005). Because of clay's poor strength, significant volumetric fluctuations, high compressibility, and swelling potential, the final product may not effectively exhibit the desired qualities. Clay behavior can be

understood in terms of its physio-mechanical characteristics as well as through other types of study, such as microstructural analysis. To distinguish between the physical and mechanical characteristics of clays before and after fire, many techniques can be applied. These include; scanning electron microscopy, thermal analysis method, and XRD method. All these characterization techniques can help us to find the components of the clays.

Several scholars have presented many models for clay particles, including Terzaghi (1925), who demonstrated that clay minerals adhere to one another at the points of contact with strong enough pressures to form a honeycomb structure. Its shape is unique to soils that include clay, and it changes according to the features of the environment.

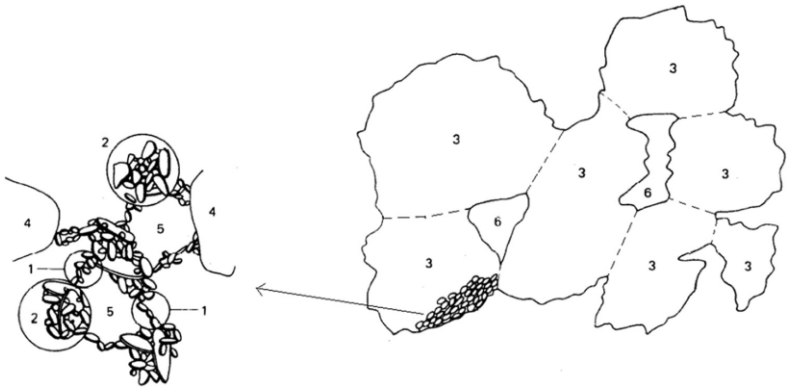

Figure 2.6: Soil Micro and Macro Fabric (Ural, 2021).

1- Structure formed by clay particles, the cluster, 2- Structure formed by the domains gathering around silt and clay and the pad is shown as clumps, 3- Among the lamps are micro spaces, which can also be selected visually, 4- The silt and sand particles, 5- Micro pores, 6- Macro pores

However, the structure of clays can be further studied by the SEM.

2.7.1: **Scanning Electron Microscopy Theory**

An essential method used to analyze the soil microstructure created by the clay particles and additives is the scanning electron microscopy. A method for producing high resolution atomic and molecular images of objects' composition, size, form and many other chemical and physical attributes is Scanning Electron Microscopy. The bonding pattern between the additives and the clay particle is identified. Materials are magnified to examine the surface differences and surface structures. The SEM visualizes electrons that are reflected as a result of an electron beam's contact with a substance. A computer connected to electron microscope as shown in figure 2.7 is used to control the microscope by capturing images which are saved in digital format.

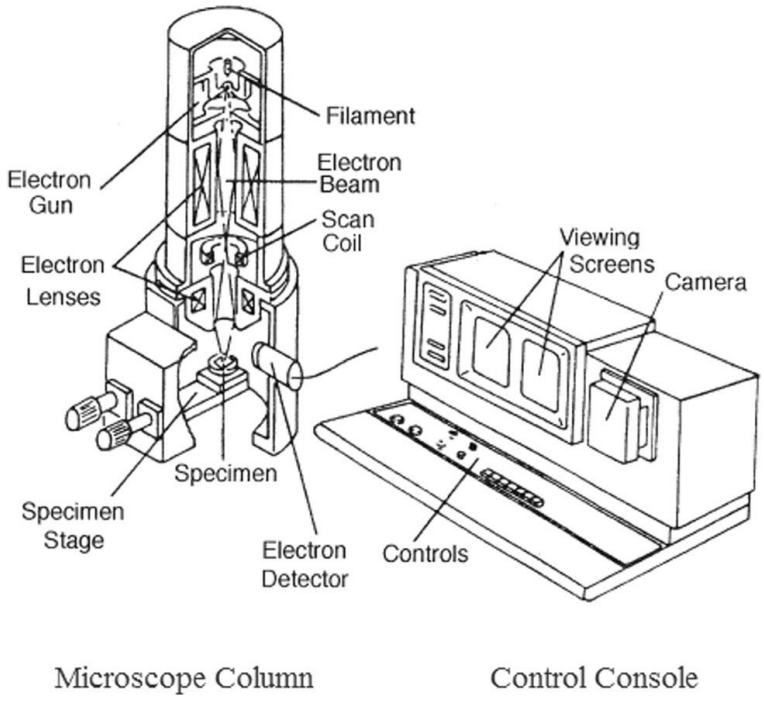

Figure 2.7: Major Parts of the SEM (Ural, 2021)

An electron beam is produced when the SEM is used in a vacuum environment. Using electromagnetic deflection coils situated in the electron column, it is then focused to a very small diameter and scanned across the surface of the specimen (sample). The position of the sample is vital since the SEM has the ability for detecting both secondary and back scattered electrons. As a result, the specimen chamber is at the bottom of the column, and the secondary electron detector is inside the specimen chamber, above the sample stage. To keep the samples stable on the scene, they are mounted using goniometers. The mobile X-ray detector is typically placed on one side of the chamber and is moved toward the sample during microanalysis. In addition, the elemental compositions of the sample can be determined using an EDX Spectrometer together with the SEM. A solid sample exposed to a focused electron beam emits an X-ray spectrum, which is employed by the Energy Dispersive Spectrometer (EDS) to provide a localized chemical analysis. The use of an X-ray spectrometer in conjunction with a scanning electron microscope might thus be crucial for obtaining electron pictures, element mapping, and point analysis (Ural, 2021).

Analysis of the quantities and qualities of specimens can be done with a point, a line and area scan all determined by Energy Dispersive Spectrometer.

In general, Scanning Electron Microscopy Analysis is done so as to help compare and explain the microstructure of samples. A microscope can be used to identify the microstructural changes in the matrix of the stabilized soil samples qualitatively.
The SEM is very useful while dealing with nanomaterials such as nanoparticles, nanowires and nanotubes. These materials are far too small to obtain detailed images using an optical microscope. With an SEM, one can see how well formed these nanomaterials are and measure their dimensions such as diameter and length. SEM has a wide range of uses, including in industry, Nano science research, biomedical testing, and microbiology. It is used in EDX spectroscopy for spot chemical analysis. The examination of minute cosmetic components also employs it. SEM may also be used to examine the topography of materials used in industry and the filament architectures of microorganisms (Ural, 2021).

The surface morphology of the raw materials refers to the size, size distribution, shape and other parameters that may help to define how the powder will flow, pack and react to form the final body. The analysis of particle sizes is a very important factor since varying their sizes directly affects the way the grains are agglomerated. The strength of a ceramic material is affected by size, shape, distribution and density or closeness of the particles. This is because these properties directly affect the texture, porosity, plasticity, specific gravity and bulk density of the ceramic material both raw and fired (Murray, 1991). The texture of the ceramic material is said to be coarse when the particles are large or loosely spaced and fine when the particles are small and closely spaced. Besides affecting the porosity and plasticity, texture also has influence on the shrinkage of the material after firing or drying. Open-textured materials whose particles are not closely packed and have many large voids are found to shrink and crack when fired or dried compared to close-texture materials with small voids and more closely packed (Kingery. W & Uhlmann, 1976).

Rahbar and Adubar.et.al (2010), report that when large particle sizes are sintered, large pore sizes are produced compared to smaller particle sizes. Due to larger pores the strength of the ceramic body formed is lower. Hutchings.et.al (2006), reported that particle size greater than 100 μm creates large pores in tiles because the particles don’t deform completely during the pressing stage and the spaces they form stay within the tile after firing. Generally finer particles create stronger fired ceramic tiles than coarse ones.

This is because they form smaller pores within the tile. Finer particles have high MOR than coarse particles as indicated in the table 2.2.

Table 2.3: Relationship between particle sizes and strength of ceramic ware.

Particle size/μm	Modulus of Rapture/MPa	Reference
45-63	68.7	(Rahbar et al., 2011)
63-90	49.8	(Rahbar et al., 2011)
90-125	35.1	(Rahbar et al., 2011)
125-250	16.6	(Rahbar et al., 2011)

Materials composed of fine particles can exhibit plastic behavior because they absorb more water than coarse particles. Firing samples made of finer particles creates many micro pores due to escaped moisture. This therefore increases linear shrinkage, warping and cracking of samples (Grimshaw & Searle, 1971). As reported by Grimshaw (1971), ceramic samples made of equal-sized particles form a system with 38 % void spaces. Maximum strength can be achieved if grading is done such that the composite material is to consist of 65.6 % of larger particles, 24.9 % of medium particles and 9.5 % of finer particles (Grimshaw & Searle, 1971). This is because maximum densification is achieved, porosity is reduced by smaller particles filling the voids hence increase in strength. The use of carefully graded materials greatly lessens the possibility of shrinking, cracking and warping when the material is subjected to sudden changes in temperature because the number of pores is reduced.

2.7.2: **X-Ray Diffraction Theory**

Using the XRD analysis technique, the atomic and molecular structure of a sample can be determined (Pandey, Dalal, Dutta, & Dixit, 2021). This technique works on the principle of exposing a sample of the material to incident X-ray beam after which the intensities and scattering angles of the x-rays that leave the sample are determined. A Graph of intensity of scattered X-rays against scattering angle is plotted and the structure of the material is determined from the analysis of the location in angle, and the intensities of scattered peaks. Figure 2.8 illustrates a schematic diagram of the principle of XRD.

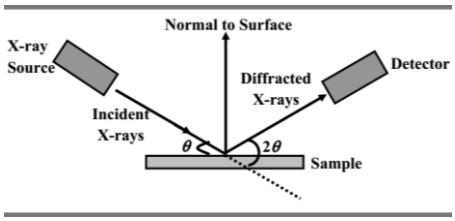

Figure 2.8: Schematic diagram for XRD process (Wubet, 2019).

The XRD analysis is used in the characterization of materials on the basis of their diffraction pattern. It is also utilized in phase identification and provides details on how internal stresses and faults cause the actual structure to differ from the ideal one. Crystals are simply defined as regular collections of atoms while X-rays are electromagnetic radiations of short wavelength. X-rays are scattered by crystal atoms through interaction with the electrons of the atoms by a phenomenon called elastic scattering in which case the electron identified as the scatterer. A regular array of scatters results in a regular array of spherical waves. According to Bragg's law, these waves build up constructively in a small number of specified directions but cancel each other out destructively in most directions:

$2d\sin\theta = n\lambda$……(1)

Where d is the distance between the atom's diffracting planes, n is an integer that represents the order of diffraction, and λ is the wavelength of the beam. The points on the diffraction pattern known as reflections represent the specific directions. Electromagnetic waves striking a regular array of scatterers cause X-ray diffraction patterns. As the wavelength of X-rays, λ, and the distance between crystal planes, d, are of a comparable order of size, they are employed to create the diffraction pattern. This non-destructive method is employed to: recognize crystalline phases and orientation; ascertain structure characteristics such as strain; grain size; phase composition; preferred orientation; and lattice parameters; measure the thickness of thin films and multi-layers; and ascertain atomic arrangement (Chauhan & Chauhan, 2014).

2.7.3: X-Ray Fluorescence Spectroscopy

Electrons are moved from their atomic orbital places during the XRF procedure, and energy unique to a particular element is released. A detector inside the device detects the energy released, and it then classifies the energy according to elements. During this

process, an x-ray beam is created by an x-ray tube which is emitted from the front end of the XRF analyzer. After interacting with the sample's atoms, it removes electrons from the atom's inner orbital shells. Electrons are displaced due to the energy gap between the primary x-ray beam produced by the analyzer and the binding energy that keeps them in their orbits. When the energy of the x-ray beam exceeds the binding energy of the electrons it interacts with, the electrons are released (Beckett, 2020). Figure 2.9 illustrates a schematic diagram of the principle of XRF.

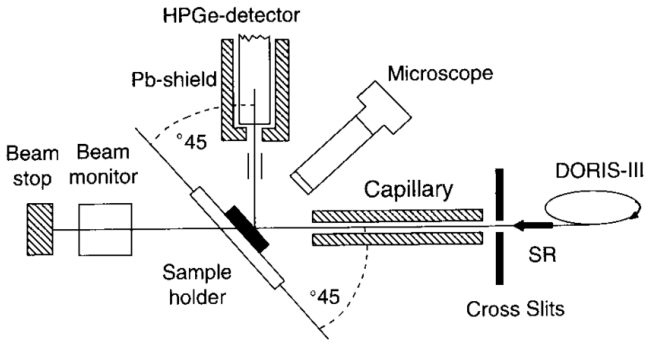

Figure 2.9: Schematic diagram for XRF process (Janssens et al., 1998).

The orbits of electrons in an atom are defined by the specific energies they possess in their orbitals. In addition, each atom possesses a unique spacing between its orbital shells; The distance between the electron shells of an atom of potassium (K) differs from that of an atom of gold (Au), silver (Ag), etc. As electrons are thrown off their orbit, voids are left behind, which destabilizes the atom. The atom then rapidly resolves this instability by filling the voids that the displaced electrons left behind. In order to fill the gaps in the lower orbit, higher orbits may travel downward. If an electron from the atom's innermost shell is knocked out of place, an electron from the next higher shell may migrate down to replace the void, emitting energy in the process. This is fluorescence.

An electron's distance from the atom's nucleus is directly proportional to its binding energy. As a result, an electron loses some energy when it moves from a higher electron shell to one that is closer to the nucleus. The energy difference between the two electron shells, which is defined by their separation, is equivalent to the amount of energy lost. Every element has a different separation between its two orbital shells. Since each element has a different quantity of energy lost during the fluorescence process, this information is utilized to identify the source element. The distinct fluorescence energies

identified correspond to the element found in the sample. The instrument or other software can calculate the ratio in which the distinct energies appear in order to ascertain the amount of each element present (Acquafredda, 2019).

CHAPTER THREE: METHODOLOGY OF STUDY

3.1: Research Design

The research design adopted here was a descriptive design in which instruments and methods were used to determine the characteristics of the raw materials used to produce the tile samples such as surface morphology, crystal structure and mineralogical composition. The second design was a correlational design to find the mechanical properties of the tile samples such as modulus of rapture and compressive strength and how they related with the composition ratios of the clay materials used.

3.2: Sample Collection of Clay

Three clay types rich in ball clay, feldspar, kaolin and sand were used to produce the tile samples. They were obtained from four different locations of Ntawo in Mukono District which is rich in ball clay, Lunya in Kayunga District which is rich in feldspar, Buwambo in Luwero District which is rich kaolin and Liddo beach in Entebbe from where sand was collected. The locations of the Ntawo ball clay deposit in Mukono District, Lunya feldspar deposit in Kayunga District, Buwambo kaolin deposit in Luwero District and Liddo beach sand deposit in Entebbe are shown in the figure 3.1. The Lunya deposit in Kayunga district is located on latitude 0.7194 ^{o}N and Longitude 32.8888 ^{o}E, approximately 40 km from Kampala on a bearing of 250 ^{o}. Liddo beach is located 34.5 km from Kampala on a latitude of 0.3960 ^{o}N and a longitude of 43.9477 ^{o}E on a bearing of 023 ^{o} from Kampala. Kaolin was collected from Buwambo village which is located in Luwero district. Ball clay was collected from Ntawo located in Mukono district in central Uganda.

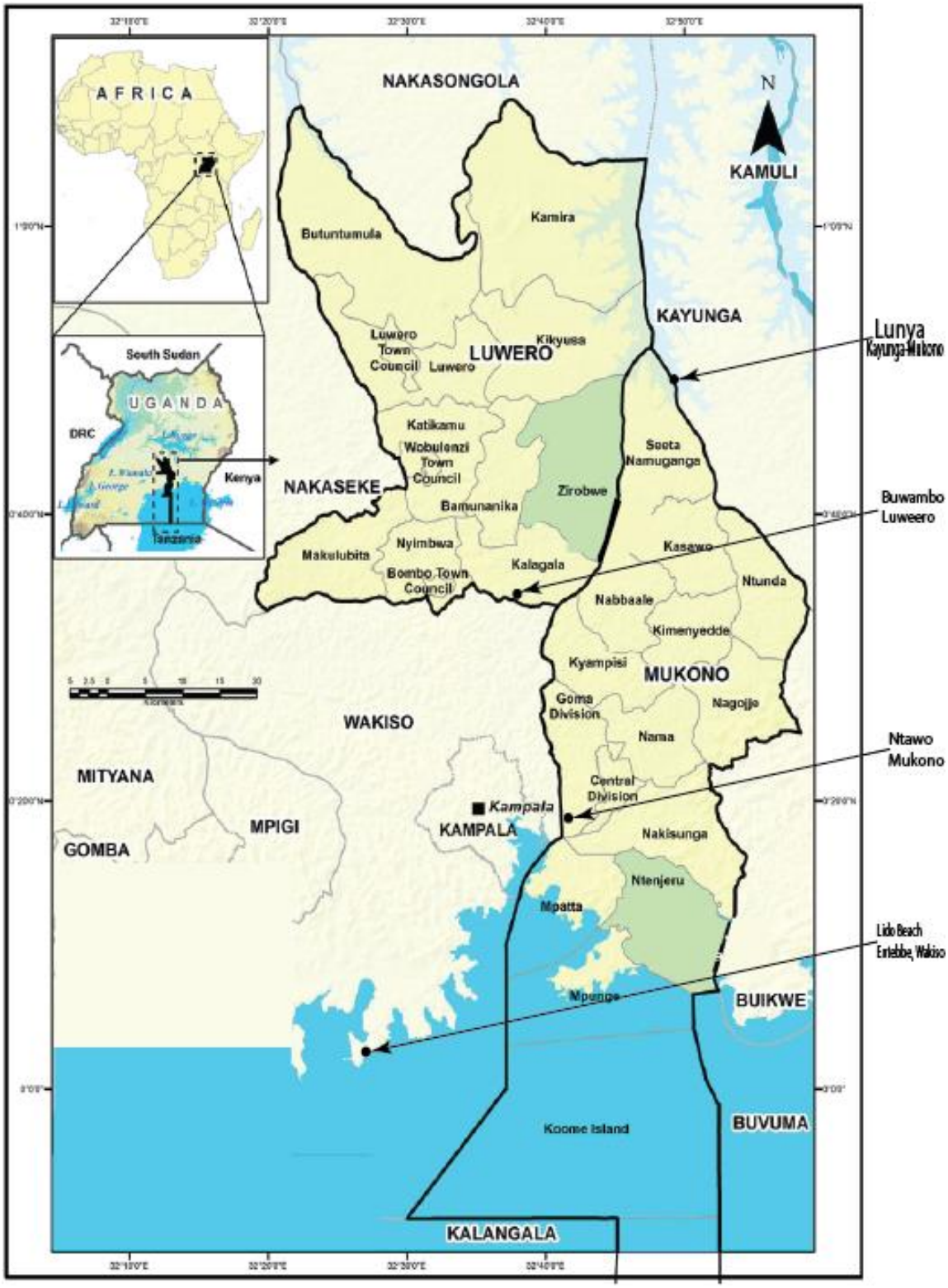

Figure 3.1: Sketch map showing the locations of Ntawo, Lunya, Buwambo and Liddo beach deposits

Each clay mineral was excavated 60 cm below the surface and weighed 300 kg. The minerals were collected, and then they were placed in polyethen bags for storage.

3.3: Preparation of Clay and Clay Mixtures

The 300 kg of Ntawo clay was soaked in 50 litres of water and stirred into a uniform paste. It was then left to settle for a week so as to allow heavy sand particles, pebbles and rock pieces to settle at the bottom and allow the light vegetative impurities such as roots, grass, and leaves to float at the top for easy removal. The clay paste was then decanted from a plastic container after removing the vegetative impurities from the top and leaving behind the heavy pebbles and stone that had settled at the bottom by gravity. The ball clay paste was then poured thinly over a flat metal surface and allowed to dry in open air inside a room for a week. The dry clay was ground in a ball mill. The milled clay was then sieved to obtain powder of particle size between 75 – 80 μm which was stored in a plastic bag.

All the kaolin rich clay was dried under the sun for five days and grounded into a powder. Impurities such as grass, stones, roots and metallic objects were removed by hand from the dried kaolin powder. The dried Kaolin powder was then dry sieved using 80 and then 75 μm sieve meshes. The sieved kaolin powder of particle size between 75 – 80 μm was placed in buckets and then covered to avoid contamination.

The feldspar rich clay was dry milled for five days using a ball mill running for ten hours each day at a speed of 50 rev/min and thereafter sieved through 80 and 75 μm sieve meshes to form white powder which was kept in plastic buckets. Porcelain milling stones got from lakes were used as the milling medium.

Sand was wet milled using a ball mill for five days running for 8 hours each day at a speed of 50 rev/min using porcelain milling stones from the lake as a milling medium. It was then wet sieved through 80 and 75 μm sieve meshes. The wet sand was then poured onto the Plaster of Paris mold and then left for five days. The semi-dried material from the Plaster of Paris mold was further dried under the sun. The dried material was then sieved to form powder of particle size between 75 – 80 μm. The powder samples were then stored in covered plastic containers.

Ball clay, kaolin, feldspar and sand were measured and mixed according to the compositions in Table 3.1 to form four different samples labeled A, B, C and D which differed in composition by percentage weight of the clays used.

Table 3.2: Masses of various clay types to make the composition ratios by % wt.

	Composition ratio (wt. %)			
Raw material	**A**	**B**	**C**	**D**
Ball clay	25	25	25	25
Kaolin	40	30	25	20
Feldspar	30	40	45	50
Sand	5	5	5	5
Total	**100**	**100**	**100**	**100**

The four mixtures A, B, C and D had the same percentage weights of ball clay and sand but different ratios of kaolin and feldspar. Sample A had kaolin - feldspar of ratio 4:3 while B had ratio of 3:4. C had ratio of 5:9 and D had a ratio of 2:5.

3.4: Production of Tile Samples

Each of the samples of A having 25 g of ball clay, 40 g of kaolin, 30 g of feldspar and 5 g of sand were mixed to form 100 g of mixture. The volume of 5 cm^3 of water was then added to the powder and then mixed for 15 minutes. Semi-dry pressing was then applied to the mixed powder and then the mixture poured into a rectangular steel mold of inner dimensions 110 mm × 50 mm × 10 mm. The mold was then placed in a jigger table for two minutes to level the content. The mold was then transferred to a compact compression machine where a force of 170 kN was applied on the mixture. The sample was then carefully removed from the mold to avoid breaking and it was left to dry in open air under a shade for one week. The mold was then cleaned before formulating another sample so as to avoid sticking of the body on the sides of the mold. A total of 25 samples of composition A were made.

Each sample of sample B was made of 25 g of ball clay, 30 g of kaolin, 40 g of feldspar and 5 g of sand were mixed to form 100 g of mixture. The above procedure for sample A was repeated until 25 sample of composition B were made. Each sample of sample C was made of 25 g of ball clay, 25 g of kaolin, 45 g of feldspar and 5 g of sand were mixed to form 100 g of mixture. The same procedure for samples A and B was repeated until 25 sample of composition C were made. To make one sample of sample D, 25 g of ball clay, 20 g of kaolin, 50 g of feldspar and 5 g of sand were mixed to form 100 g of

mixture. The same procedures for A, B and C were repeated until 25 sample of composition D were made.

The dried samples of A, B, C, and D were heated in batches from room temperature to 105 ^{o}C at a firing rate of 2 ^{o}C per minute. This helped to drive off moisture before actual firing takes place without causing rapid and potentially damaging expansion due to steam formation. The temperature was then increased to 360 ^{o}C and held there for one hour and then increased to peak temperature of 1100 ^{o}C and held there for 50 minutes. Maintaining the temperature of the tiles at 360 ^{o}C for one hour allows for the thorough removal of chemically bound water contained in the raw materials that could turn into steam during later stages of firing, leading to defects like cracks or warping. Maintaining the temperature of the tiles at 1100 ^{o}C for 50 minutes allows for the optimal sintering (process where the ceramic particles fuse together) of the ceramic particles thus promoting a dense, solid structure. The fired tiles were then kept in the kiln before switching off the firing kiln. The tile samples were then left to cool down to room temperature before removing them. The samples were then kept in buckets labeled A, B, C, and D ready for further testing and measurements.

3.5: Characterization of Raw Clay Materials

The surface morphology, crystal structure and mineralogical composition of raw ball clay, feldspar, kaolin and sand were determined.

3.5.1: Surface Morphology Analysis of Raw Materials

The surface morphology analysis of the raw materials used to produce the tile samples were investigated by the Scanning electron microscopy. The raw materials were crashed into fine powder. They were then put into the SEM chamber for analysis. The SEM gave the images for each raw material fed into it. The pictures were analyzed to give the morphology of the four raw materials.

3.5.2: Crystal Structural Analysis of Samples

Structural analysis of the raw clay materials was done using XRD of wavelength 0.15418 nm. The powders for each clay was placed on glass substrate and inserted into the machine. The XRD gave diffraction data of intensity and diffraction angle. The data was analyzed to determine the different mineral phases such as kaolinite present in the samples.

3.5.3: Mineralogical Composition of Samples

The mineralogical composition of the raw materials was investigated using EDX Spectroscopy and XRF. The raw materials were crashed into powder and placed on a carbon coated tape. Powders of kaolin, feldspar and ball clay were analyzed using EDX. Sand was analyzed for silica and other chemical compounds using XRF. During analysis, the sample was ground to fine powder (< 0.063) from which pressed powder pellets was made and scanned using an XRF spectrometer (Epsilon 1). The results obtained were expressed in percentage weight (wt. %) of the compounds present in the sample.

3.6: Measurement of Mechanical Properties of Tile Samples

The experimental measurements of the tile samples focused on the CS and MOR of the tile samples. The measurement of these properties was carried out from Uganda National Bureau of Standards at UIRI laboratory.

3.6.1: Modulus of Rapture of Tile Samples

To determine the MOR, five tile samples from each composition were used. The MOR was measured using a universal MOR testing equipment. The three-point loading test was done. The machine was adjusted by moving two lower cylindrical rods so that they are of equal length from both ends of the sample. Three points were marked on each sample where the cylindrical rods were placed. The span distance L between two lower cylindrical rods was adjusted to 70 mm. The loading force was applied at a rate of 2 mm/min directed to the center of the fired sample. The force was applied until the sample brakes.

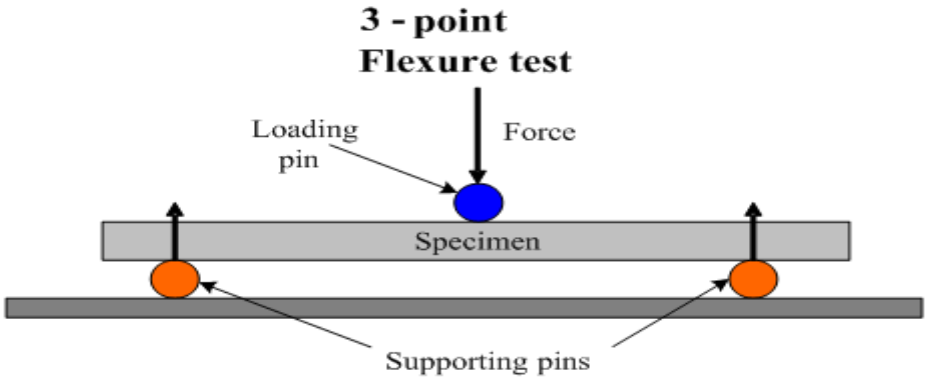

Figure 3.2: Three Point Setting on Sample

The scale reading at this point was then recorded. After each reading, the scale was re-set to zero before another measurement was taken. The proving ring reading was multiplied by a constant to obtain the loading force, F, in kN. The modulus of rapture was calculated from the equation1 (Ochen, 2012).

$$MOR = \frac{3FL}{2bt^2} \quad \text{.....(1)}$$

where F is the breaking force, b is the breadth and t is the thickness of the sample. The values of modulus of rapture were calculated and recorded.

3.6.2: Compressive Strength of Tile Samples.

To determine the CS, five tile samples from each composition were used. The CS of the tile samples was measured using CS testing equipment shown in figure 3.3.

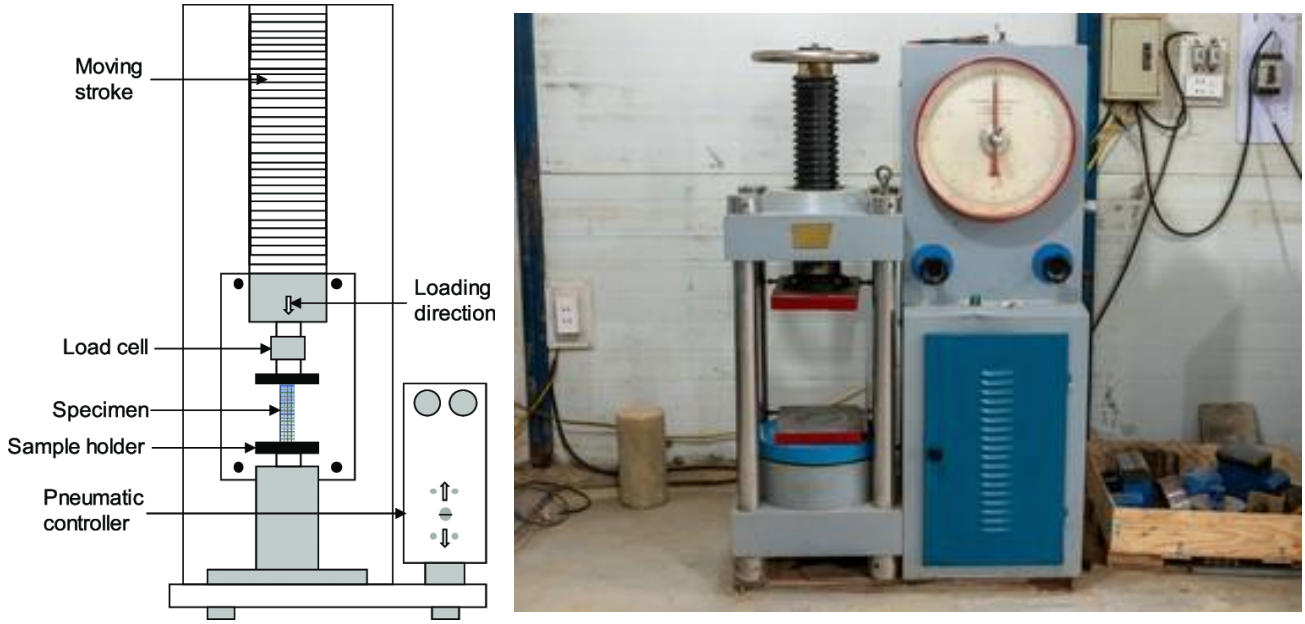

Figure 3.3: Compressive Strength testing equipment

The Compressive strength, CS, of the samples was obtained from the equation 2 by dividing the force, F, at point of failure with the initial cross-sectional surface area, A, of the samples (Ochen, 2012).

$$cs = \frac{F}{A} \quad \text{.....(2)}$$

The dimensions of the samples including thickness, t, breadth, b, and length, L, were measured using a vernier caliper from which the cross-sectional area was obtained. The values of CS were recorded.

CHAPTER FOUR: RESULTS OF THE STUDY

4.1: Introduction

This study was designed to give five results of surface morphology, crystal structure, mineralogical composition of raw materials used to produce the tiles and two mechanical properties namely, modulus of rapture and compressive strength of the developed tiles. This chapter covers the results and the discussions of crystal structure, mineralogical composition and surface morphology of the raw clay materials which were done using X-Ray Diffractometry, Energy Dispersive X-ray (EDX) Spectroscopy / XRF and Scanning Electron Microscopy respectively. Furthermore, the results of the MOR and CS of the tiles developed using the testing equipments have also been presented and discussed.

4.2: Characterization of Clay Raw Materials

This involved coming up with surface morphology, crystal structure and mineralogical composition of the raw minerals used in this study.

4.2.1: Surface Morphology Analysis of the Raw Materials

This was done using the SEM described in 3.5.1. The results obtained are presented below.

(a) Buwambo Kaolin.

The surface morphology of kaolin clay used in this study is shown in figure 4.1.

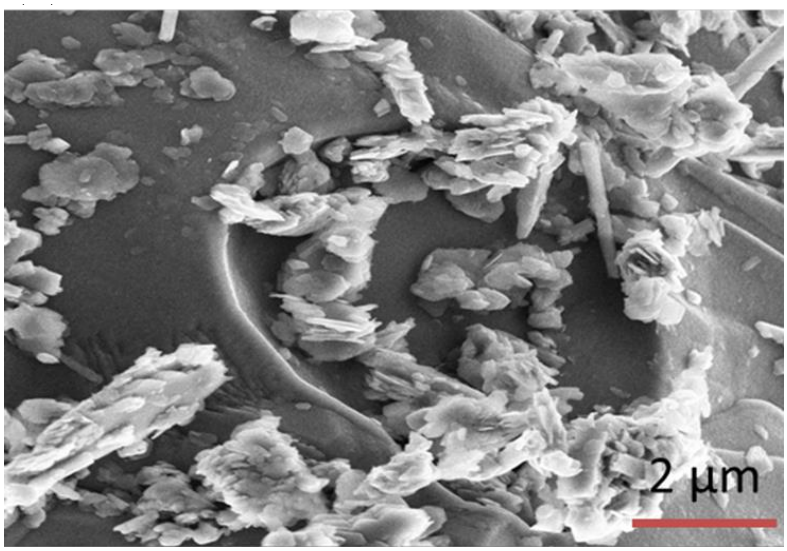

Figure 4.1: SEM Image of Kaolin

(b) Lunya Feldspar.

The surface morphology of Lunya feldspar used in this study is shown in figure 4.2

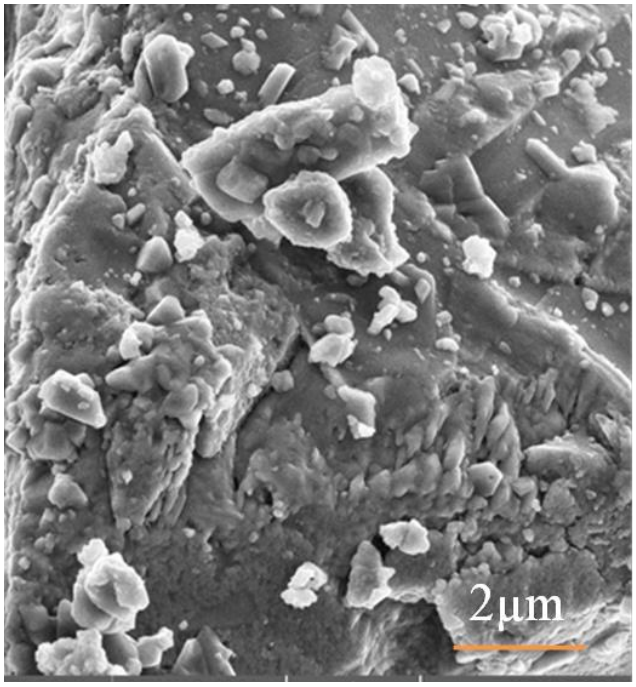

Figure 4.2: SEM image of Feldspar

(c) Ntawo Ball Clay.

The surface morphology of Ntawo ball clay used in this study is shown in figure 4.3

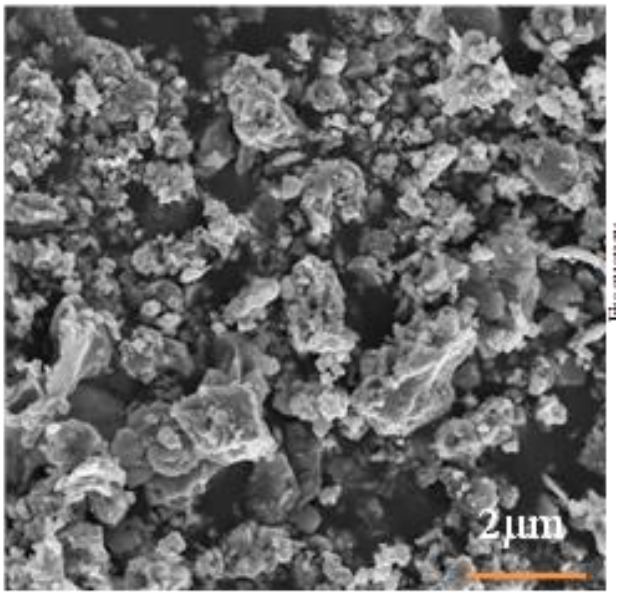

Figure 4.3: SEM of Ball Clay

(d) Liddo Beach Sand

The surface morphology of Liddo beach sand used in this study is shown in figure 4.4

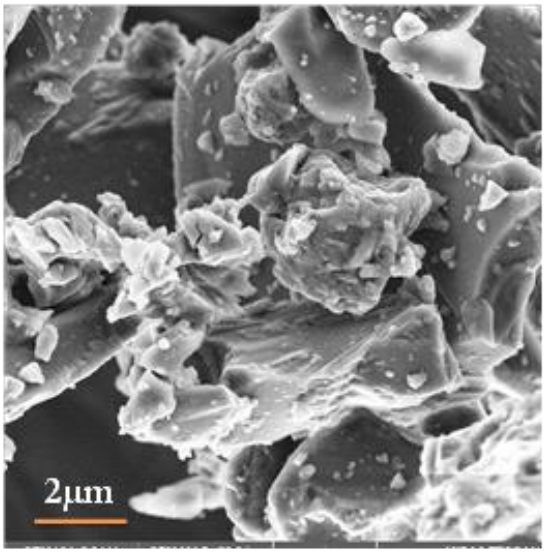

Figure 4.4: SEM image of Sand

4.2.2: Crystal Structural Analysis of Raw Materials (XRD Results)

The crystal structure of kaolin, ball clay, sand and feldspar minerals were identified by comparing the position of the peak intensity (2θ) in the samples with the standard peak position value of the diffraction intensity (2θ). A graph of intensities of scattered X-rays against scattering angle was plotted and the structures of the materials were determined from the analysis of the location, in angle, and the intensities of scattered peaks.

(a) Kaolin.

The XRD patterns obtained for kaolin are shown in figure 4.7

.

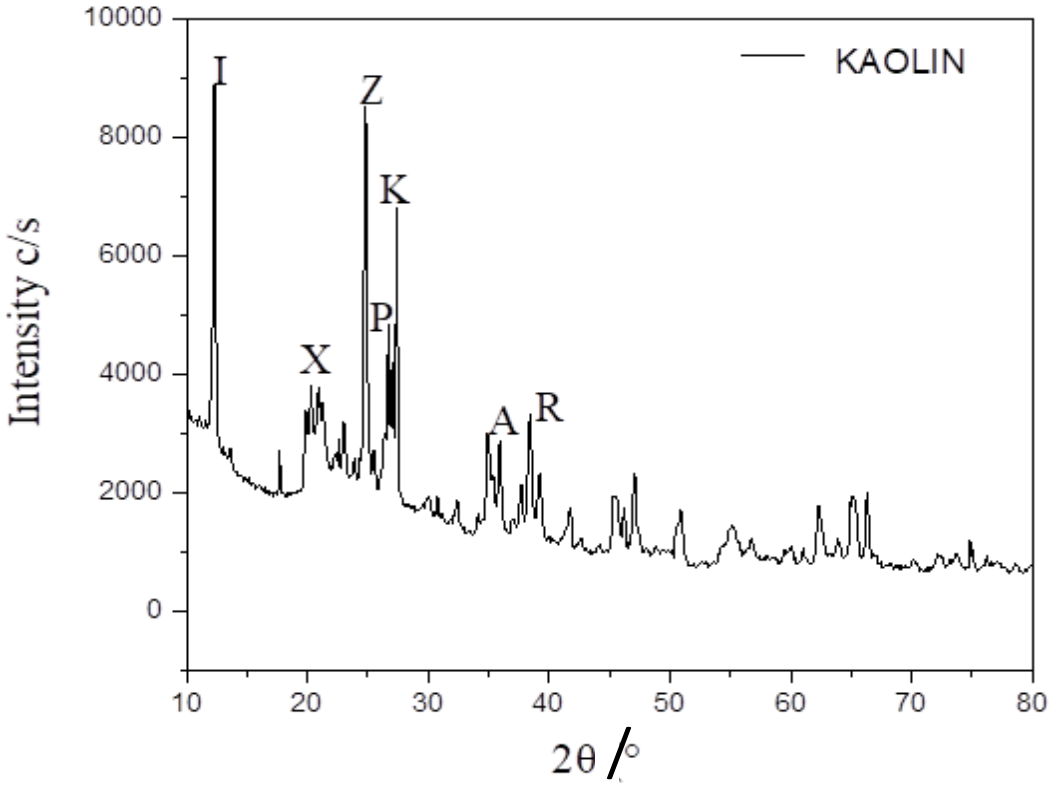

Figure 4.5: X-ray Diffractogram of kaolin

The values of inter atomic spacing, d (Å) obtained in this study were calculated using $d = \frac{n\,\lambda}{2\,sin\theta}$ where d is the spacing between diffracting planes of the atoms, θ is the diffraction angle, n is an integer which is the order of diffraction, and λ is the beam wavelength (Wavelength of x-rays used 1.5418 Å). The calculated d values are shown in table 4.1

Table 4.1: Values obtained for interatomic spacing (d) for Kaolin

2θ / °	θ / °	d / Å (Experimental)	d / Å (Literature) (Dewi, Agusnar, & Alfian, 2018)
12.29	6.15	7.19	7.14
20.31	10.15	4.38	-
24.80	12.40	3.59	3.57
26.70	13.35	3.34	-
27.40	13.70	3.23	2.34
35.89	17.95	2.50	-
38.39	19.19	2.35	-
41.73	20.87	2.16	-
46.89	23.45	1.94	-
66.31	33.16	1.41	-

(b) Ball Clay

The XRD patterns obtained for ball clay are shown in figure 4.6.

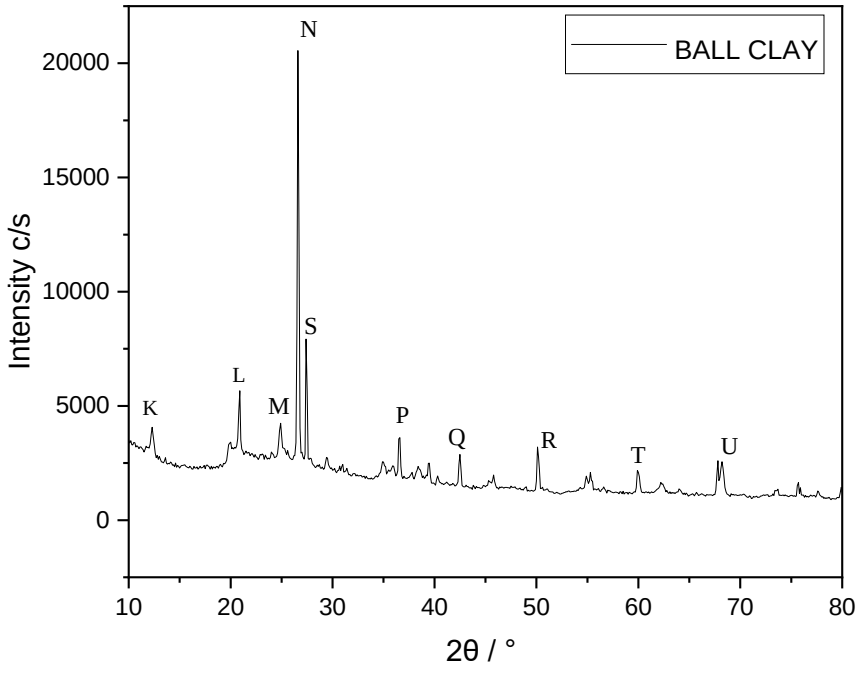

Figure 4.6: X-ray Diffractogram of Ball Clay

The values of inter atomic spacing, d (Å) obtained in this study for ball clay were calculated as shown in table 4.2.

Table 4.2: Values of Interatomic Spacing (d) for Experimental and Literature Ball Clay

2θ / °	θ / °	d /Å (Experimental)	d / Å (Literature) (Dewi et al., 2018)
12.27	6.14	7.21	7.14
20.82	10.41	4.27	-
25.03	12.52	3.56	3.36
26.53	13.27	3.36	-
27.35	13.68	3.26	-
36.84	18.42	2.44	2.34
42.41	21.21	2.13	-
49.88	24.94	1.83	-
60.07	30.04	1.54	-
68.08	34.04	1.38	-

(c) Sand

The XRD patterns obtained for silica are shown in figure 4.7.

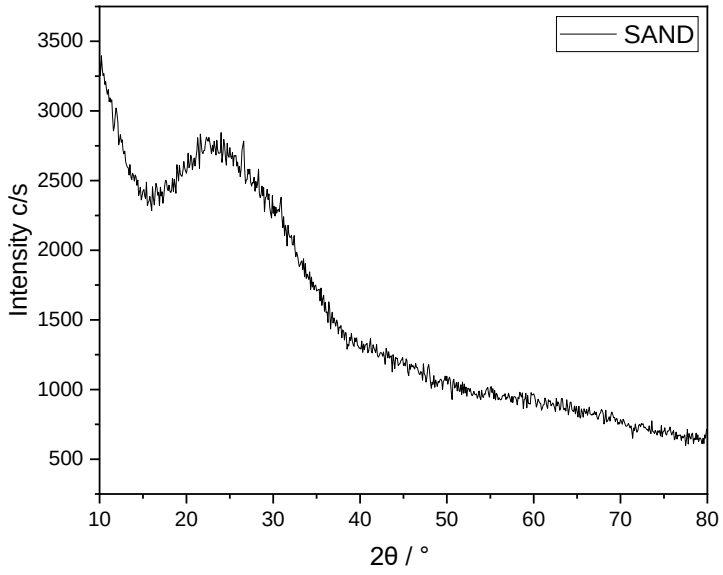

Figure 4.7: X-ray diffractogram of Sand

(d) Feldspar

The XRD patterns obtained for feldspar are shown in figure 4.8.

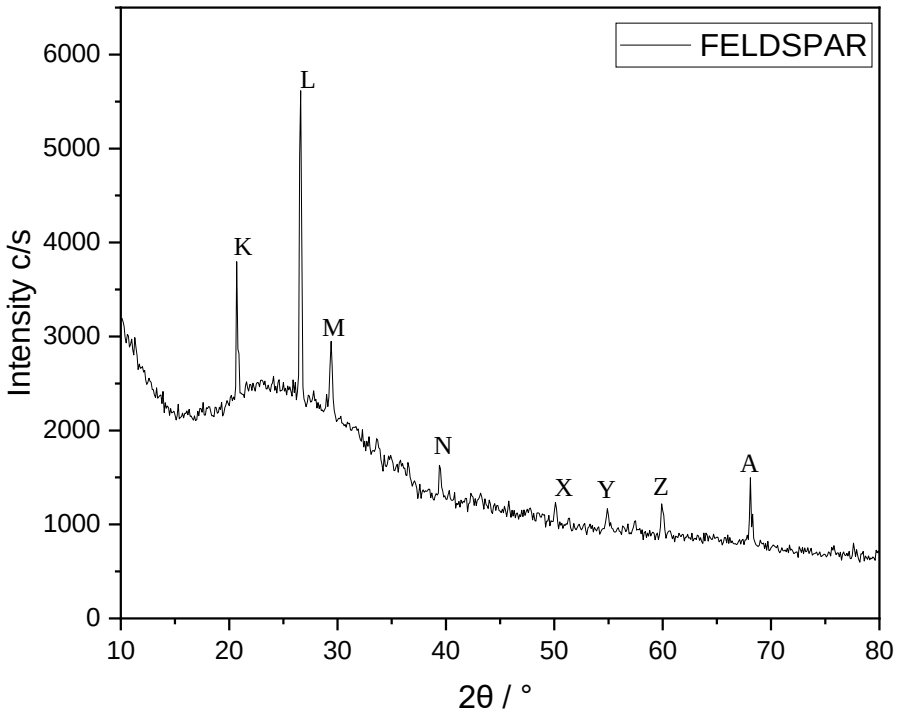

Figure 4.8: X-ray Diffractogram of Feldspar used

The obtained values of inter atomic spacing, d (Å) for feldspar used in this study were calculated as shown in table 4.3.

Table 4.3: Values of Interatomic Spacing (d) for Experimental and Literature Feldspar

2θ / °	θ / °	d / Å (Experimental)	d / Å (Literature) (Lewicka & Trenczek-Zajac, 2020)
20.69	10.35	4.29	4.26
26.40	13.20	3.38	3.48
29.52	14.76	3.03	3.24
39.43	19.72	2.28	-
50.28	25.14	1.81	-
54.77	27.40	1.68	-
60.21	30.11	1.54	-
67.93	33.97	1.38	-

4.2.3: Mineralogical Composition of Raw Materials using EDX and XRF.

(a) Kaolin

The mineralogical composition of kaolin was characterized by Energy Dispersive X-ray Spectroscopy. The sampling areas and EDX spectra are shown in figure 4.9 (a) and (b) respectively. The EDX spectra shows the number of detected photons(counts) against wavelength in energy(keV).

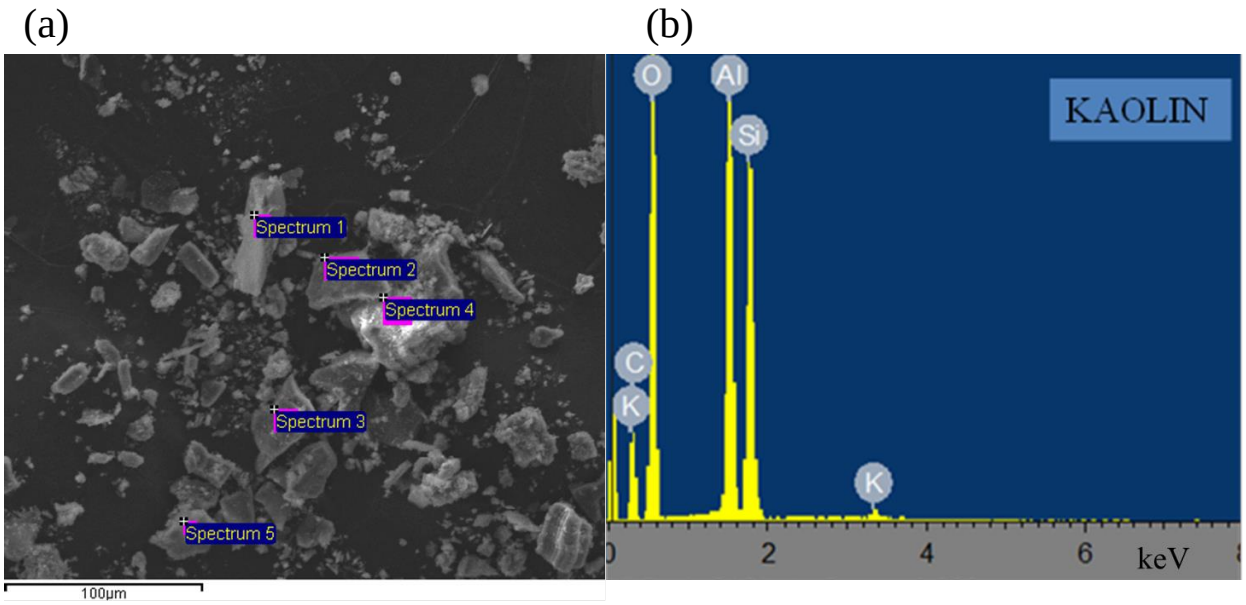

Figure 4.9: (a) Sampling areas and (b) EDX spectra of kaolin.

The ratios of various elements present in kaolin are summarized in table 4.4.

Table 4.4: Ratios of various elements present in kaolin

Ratio		
Si/Al	Si/O	Al/O
0.97	0.21	0.22

(b) Ball Clay

The mineralogical composition of ball clay was characterized by Energy Dispersive X-ray Spectroscopy. The sampling areas and EDX spectra are shown in figure 4.10 (a) and (b) respectively.

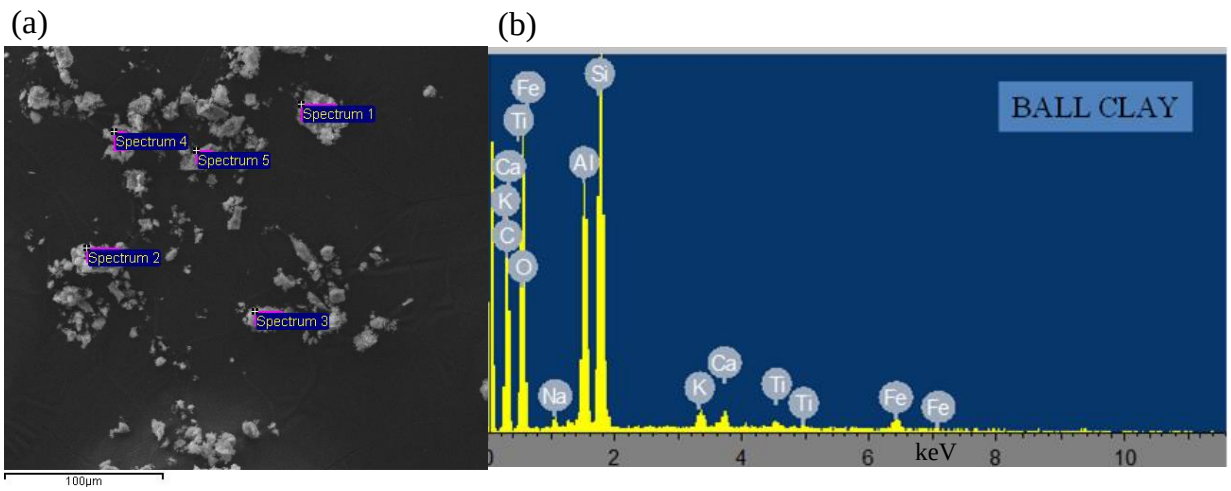

Figure 4.10: (a) Sampling areas and (b) EDX spectra of Ball Clay.

The percentages of the elements present in experimental ball clay were determined from the Energy Dispersive Spectrometer spectra as indicated in table 4.5.

Table 4.5: Elemental composition (Wt. %) of experimental Ball clay

Elements Present	**Weight (%)**
O	45.53
Si	12.91
Al_2	4.52
C	34.8
Fe	0.86
Ti	0.30
Ca	0.41
K	0.28
Na	0.39

The EDX results for experimental ball clay matched with its XRD results.

(c) Feldspar

The mineralogical composition of feldspar was characterized by EDX. The sampling areas and EDX spectra are shown in figure 4.11 (a) and (b) respectively.

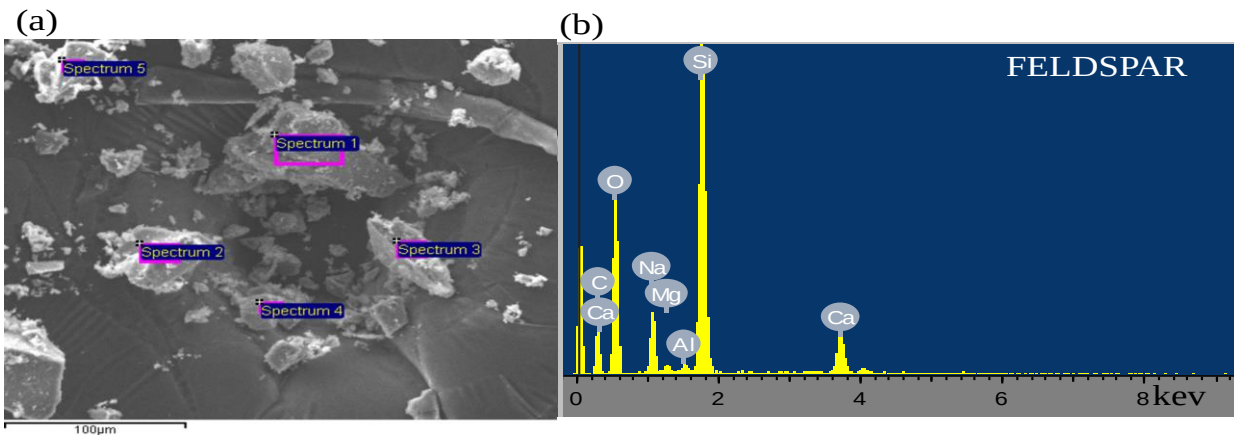

Figure 4.11: (a) Sampling areas and (b) EDX spectra of Feldspar.

The ratios of the atomic concentrations of the elements of feldspar were determined from the Energy Dispersive Spectrometer spectra as shown in table 4.6.

Table 4.6: Ratio of various elements present in feldspar

Ratios	
Ca/Na	Na/Ca
0.71	1.40

(d) Sand

The mineralogical composition of sand was characterized by XRF. The percentage weight of these oxides is indicated in table 4.7.

Table 4.7: Chemical composition (Wt. %) of sand

Oxides Present	**Weight (%)**
SiO_2	99.5.
Al_2O_3	0.2
Fe_2O_3	0.2

4.3: Mechanical Properties of Tiles Produced

The MOR and CS were the mechanical properties tested for the tiles produced for the four mixture ratios A **(**5:8:6:1), B **(**5:6:8:1), C **(**5:5:9:1) and D **(**5:4:10:1) whose optical image after firing are shown in figure 4.12.

Figure 4.12: Optical image of tile samples A, B, C and D after firing whose mold dimensions were 110 mm × 50 mm × 10 mm.

Tile A has a brownish rough like texture followed by tile B, C and D. The reaction between kaolin and feldspar resulted into the diffusion of more iron particles in ball clay forming the brownish color in tile sample A and B as compared to C and D.

4.3.1: Modulus of Rapture (MOR) of Sample Types

Appendix B and E show the statistical data for MOR of the tile samples. The MOR of the tile samples for the four compositions were calculated using equation (1) and recorded as shown in the table 4.8. The table also indicates the mean, standard deviation and the maximum error of estimate at confidence levels or significant levels of $\alpha = 0.01$ and $\alpha = 0.05$.

Table 4.8: MOR of Tile samples for the four compositions, A, B, C and D

Composition Ratios	A	B	C	D
Mean MOR / MPa	30.836	27.780	23.788	18.580
Standard Deviation	1.775	1.061	1.169	0.341
Maximum Error at $\propto = 0.01$	2.672	1.597	1.759	0.512
Maximum Error at $\propto = 0.05$	1.599	0.956	1.054	0.307

A bar chart of MOR against composition ratios was plotted in order to show the variation in MOR of the tile samples with composition ratios as shown in figure 4.13.

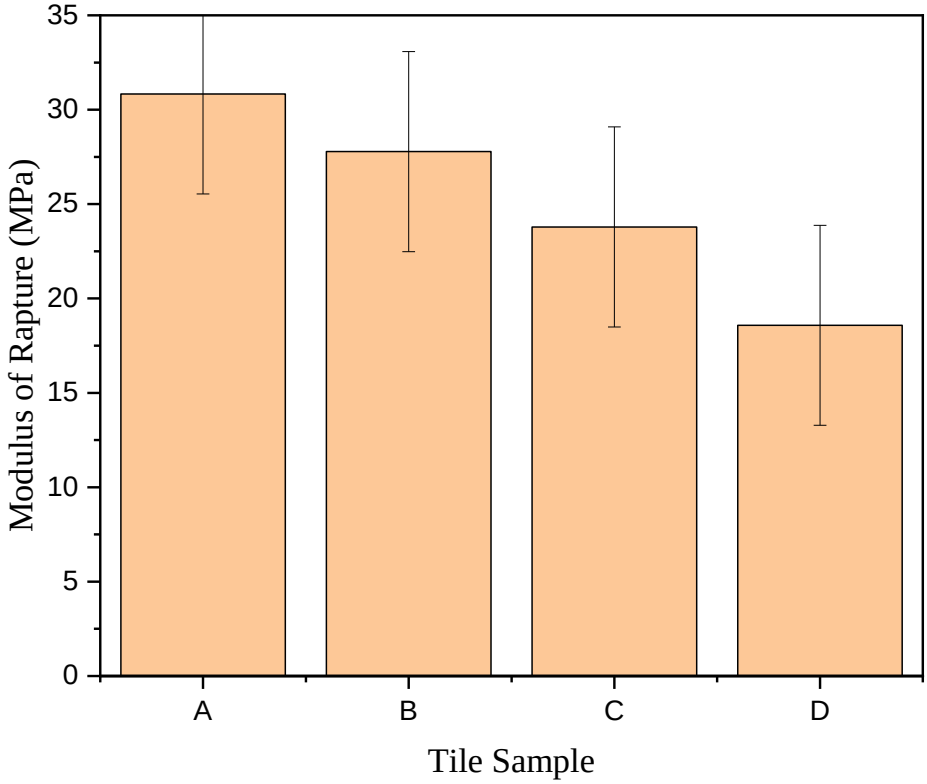

Figure 4.13: Bar chart of MOR of tile samples of different composition ratios (Origin)

The variation in the MOR with composition was tested using the F-test. The F- test was performed in order to determine if the MOR for the tile samples above were statistically different for the different compositions. The calculated F-value and the critical values at confidence levels of $\alpha = 0.01$ and $\alpha = 0.05$ were obtained as shown in the table 4.9.

Table 4.9: The F values for the tile samples

Calculated F-value	Critical F value at $\alpha = 0.05$ (from table)	Critical F value at $\alpha = 0.01$ (from table)
102.802	3.24	5.29

It was clearly seen that the calculated F-value of 102.802 and the critical F-values (table values) of 3.24 and 5.29 at $\alpha = 0.05$ and $\alpha = 0.01$ respectively were statistically different. The calculated F-value was greater than the critical F-values. This implied that at both

levels of significance, the composition ratios were significantly different implying that each composition ratio had a different MOR. The null hypothesis that the modulus of rapture of the tiles produced will not be affected by the composition ratios of the clay mixture is rejected at the two levels of significance. The MOR is thus significantly affected by composition ratios at the two levels of significance.

Composition A had the highest mean value of MOR of 30.836 MPa while composition D had the lowest mean value of MOR of 18.58 MPa.

The range for the highest MOR i.e. the difference between the mean value and the error of estimate at $\alpha = 0.01$ and $\alpha = 0.05$ were calculated as shown below.

Range at $\alpha = 0.01$; 30.836 + 2.672 = 33.51 MPa and 30.836 - 2.672 = 28.16 MPa

Range at $\alpha = 0.05$; 30.836 + 1.599 = 32.44 MPa and 30.836 - 1.599 = 29.24 MPa

The highest MOR at $\alpha = 0.01$ was found to be in the range of 28.16 MPa to 33.51 MPa and 29.24 MPa to 32.44 MPa at $\alpha = 0.05$

The range for the lowest MOR i.e. the difference between the mean value and the error of estimate at $\alpha = 0.01$ and $\alpha = 0.05$ were calculated as shown below.

Range at $\alpha = 0.01$; 18.580 + 0.512 = 19.09 MPa and 18.580 - 0.512 = 18.07 MPa

Range at $\alpha = 0.05$; 18.580 + 0.307 = 18.89 MPa and 18.580 – 0.307 = 18.27 MPa

The lowest MOR at $\alpha = 0.01$ was found to be in the range of 18.07 MPa to 19.09 MPa and 18.27 MPa to 18.89 MPa at $\alpha = 0.05$

4.3.2: **Compressive Strength (CS) of Sample Tiles**

The CS of the tile samples for the four compositions were calculated using equation (2) and recorded as shown in the table 4.10. The table also indicates the mean, standard deviation and the maximum error of estimate at confidence levels or significant levels of $\alpha = 0.01$ and $\alpha = 0.05$.

Table 4.10: CS of tile samples for the four compositions, A, B, C and D

Composition Ratios	A	B	C	D
Mean CS / MPa	1.358	1.074	1.018	0.818
Standard Deviation	0.039	0.023	0.033	0.018
Maximum Error at $\propto = 0.01$	0.059	0.035	0.050	0.027
Maximum Error at $\propto = 0.05$	0.035	0.021	0.030	0.016

A bar chart of CS against composition ratios was plotted in order to show the variation in CS of the tile samples with composition ratios as shown in figure 4.14.

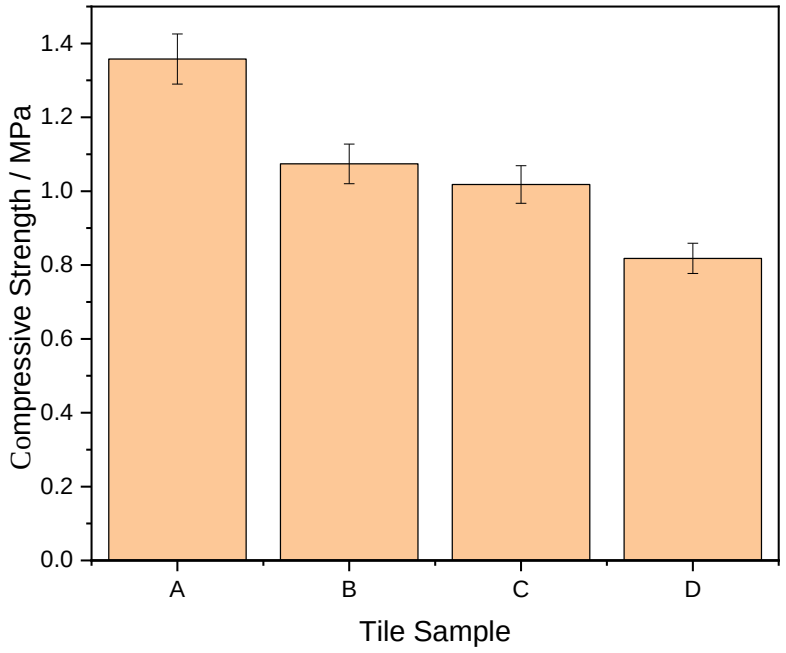

Figure 4.14: Bar chart of CS of tile samples of different composition ratios (Origin)

Tile sample A has the highest CS followed by B, C and D had the least compressive strength.

The variation in the CS with composition is statistically supported using the F-test. The F- test was performed in order to determine if the CS for the tile samples above were statistically different for the different compositions. The calculated F-value and the critical values at confidence levels of $\alpha = 0.01$ and $\alpha = 0.05$ were obtained as shown in the table 4.11.

Table 4.11: The F values for the tile samples

Calculated F-value	Critical F value at α= 0.05 (from table)	Critical F value at α= 0.01 (from table)
290.21	3.24	5.29

It was clearly seen that the calculated F-value of 290.21 and the critical F-values (table values) of 3.24 and 5.29 at α= 0.05 and α= 0.01 respectively were statistically different. The calculated F-value was greater than the critical F-values. This implied that at both levels of significance, the composition ratios were significantly different implying that each composition ratio had a different compressive strength. The CS for the four compositions was statistically different. The null hypothesis that the CS of the tiles produced will not be affected by the composition ratios of the clay mixture is rejected at the two levels of significance. The CS is thus significantly affected by composition ratios at the two levels of significance.

Composition A had the highest mean value of compressive strength of 1.358 MPa while composition D had the lowest mean value of compressive strength of 0.818MPa.

The range for the highest CS i.e. the difference between the mean value and the error of estimate at α= 0.01 and α= 0.05 were calculated as shown below.

Range at α = 0.01; 1.358 + 0.059 = 1.417 MPa and 1.358 - 0.059 = 1.299 MPa

Range at α = 0.05; 1.358 + 0.035 = 1.393 MPa and 1.358 - 0.035 = 1.323 MPa

The highest CS at α = 0.01 was found to be in the range of 1.299 MPa to 1.417 MPa and 1.323 MPa to 1.393 MPa at α = 0.05

The range for the CS i.e. the difference between the mean value and the error of estimate at α = 0.01 and α = 0.05 were calculated as shown below.

Range at α = 0.01; 0.818 + 0.027 = 0.845 MPa and 0.818 – 0.027 = 0.791 MPa

Range at α = 0.05;

0.818 + 0.016 = 0.834 MPa and 0.818 – 0.016 = 0.802 MPa

The lowest CS at $\alpha = 0.01$ was found to be in the range of 0.791 MPa to 0.845 MPa and 0.802 MPa to 0.834 MPa at $\alpha = 0.05$

CHAPTER FIVE: DISCUSSION, CONCLUSIONS AND RECOMMENDATIONS

5.1: Introduction

This chapter has covered the discussion of the results of the study. The findings have also been compared with similar studies done in Uganda and world over. Possible conclusions and recommendations have been drawn.

5.2: Discussion of Results of the Study

There are five areas of the results covered in this discussion. The surface morphology of the raw materials used to produce the tiles, the crystal structural of raw materials, the mineralogical composition of raw materials, the modulus of rapture and compressive strength of sample tiles.

5.2.1: Surface Morphology Analysis of the Raw Materials

The kaolin particles were found to be irregular in shape with a porous texture. In addition, the particles were agglomerated of average particle size of approximately 0.202 ± 0.131 μm. It was observed that the feldspar samples showed an irregular surface morphology of particles with average particle size of approximately 0.153 ± 0.105 μm. In addition, some small feldspar particles were observed. The SEM image for ball clay showed agglomerated particles of average size approximately 0.095 ± 0.055 μm which were fine grained and uniformly rounded crystals in form of pockets between kaolinite fragments. The SEM image of silica displays the silica particles in an agglomerated form. It also displayed fine silica particles with a porous agglomerated texture with average particle size of approximately 0.168 ± 0.198 μm. The aggregates had a similar shape to one another.

5.2.2: Crystal Structural Analysis of Raw Materials (XRD Results)

According to the XRD results for the kaolin used in this study, the scattering/diffraction peaks were located at 2θ / ° = 12.29, 20.30, 24.80, 26.70, 27.40, 35.89, 38.39, 41.73, 46.89 and 66.31 ° as indicated by the letters I, X, Z, P, K, A and R on the XRD graph. Major peaks were located between 12.29 and 27.40 ° as shown in figure 4.5 and were

similar to literature major peaks for kaolin located between 12.26 to 24.81 ° as observed by Dewi. (Dewi et al., 2018)

From table 4.1, it was noticed that the d-values of experimental kaolin highly correlates with the literature values. Hence confirming further that the material used in this study was that of kaolin.

Furthermore, kaolin is a mineral composed of silica (SiO_2) and alumina (AL_2O_3) as the major mineralogical constituents. Studies show that the 2θ value for standard silicate (SiO_2) pattern lies between 20.0 and 25.0 ° (Joni, Nulhakim, Vanitha, & Panatarani, 2018). In the current study, the peaks observed at 20.31 ° and 24.8 ° corresponded to silica as were observed by other researchers in literature (Joni et al., 2018).

Studies also show that the 2θ value for standard alumina (AL_2O_3) pattern lies at 36, 45.79 and 67.3 °. In the current study, the peaks observed at 46.89 ° and 66.31 ° corresponded to alumina as was observed by other researchers in literature (Kanwal, Batool, Adnan, & Naseem, 2015). Other peaks observed could correspond to potassium oxide (K_2O) and were due to impurities present in kaolin since the sample used was impure. On comparison of the XRD results obtained with those in literature, it was confirmed that the kaolin used in this study was a kaolinite mineral compound whose major mineralogical constituent compounds were silica (SiO_2) and alumina (AL_2O_3).

According to the XRD for ball clay used in this study, the scattering peaks were located at 2θ / ° = 12.27, 20.82, 25.03, 26.53, 27.35, 36.84, 42.41, 49.88, 60.07 and 68.08 as indicated by the letters K, L, M, N, S, P, Q, R, T and U on the XRD graph. Major peaks were obtained at 20.82, 26.53 and 27.35 ° as shown in figure 4.6. From literature, standard Ball clay has kaolinite as the main mineral (Baioumy & Ismael, 2014). The diffractogram for standard kaolin and that of ball clay used in this study were compared and they showed proximity. Therefore, the clay used in this study was ball clay. From table 4.2, it was noticed that the d-values of experimental ball clay seemed to agree with the literature values for kaolinite mineral hence confirming further that the material used in this study was that of ball clay. Other peaks observed revealed impurities present in ball clay used since it was impure.

The diffraction patterns for silica indicated a broad peak at 2θ = 22.86 °. A similar peak was obtained at 2θ = 22 ° by Nallathambi et al which revealed the amorphous nature of

the silica nanoparticles (Nallathambi, Ramachandran, Venkatachalam, & Palanivelu, 2011). On comparison of the values of absorption peaks of the silica used in this study with those of standard amorphous silica nanoparticles, they showed proximity hence confirming that the silica used was amorphous and hence lacked any ordered crystalline structure.

According to the XRD results for feldspar used in this study, the scattering peaks were located at 2θ / ° = 20.69, 26.40, 29.52, 39.43, 50.28, 54.77, 60.21 and 67.93 as indicated by the letters K, L, M, N, X, Y, Z and A on the XRD graph. Major peaks are located at 20.69, 26.40 and 29.52 ° as shown in figure 4.8. From literature, major peaks for standard sodium feldspar were located at values between 25.0 ° to 30.0 ° as obtained by Halmurat. (Halmurat, Yusufu, Wang, He, & Sidike, 2019). Therefore, the XRD diffractogram for standard sodium feldspar and that of the feldspar used in this study showed proximity compared to the diffractograms for Potassium and Calcium feldspar. Therefore, the feldspar used in this study was sodium feldspar.

It was observed from table 4.3 that the d values for standard feldspar and those for feldspar used in this study showed proximity. These results obtained clearly showed that the feldspar used in this study was that of Sodium Aluminium Silicates **(**$NaAlSi_3O_8$) feldspar.

5.2.3: Mineralogical Composition of Raw Materials using EDX and XRF.

The observed kaolin peaks included potassium, oxygen, aluminium and silicon. It was observed that the peak for oxygen was higher than that of aluminium. The Aluminium peak was however slightly higher than that of silicon. The summary of elemental distribution in kaolin using EDX is shown in table 4.4. Furthermore, the average percentage by mass of kaolin based on five (5) measurements were obtained through quantitative analysis and these were 51.61% for oxygen, 11.15% for Aluminium, 10.83% for Silicon and 0.43% Potassium as summarized in table 4.4.

From literature, the ratio of aluminium to silicon must be close to one (1) for a kaolinite mineral (Pinet, Lartiges, Martinez, & Ouillon, 2019). As observed from table 4.4, the ratio of Si: Al was 0.97 ~ 1 which seemed to agree with the literature value for kaolinite thus confirming further that the mineral used was that of kaolin. The Experimental kaolin had mostly oxides of aluminium and silicon with very small percentage of potassium.

The ratio of silicon to aluminium in the kaolin was ~ 1:1. The results indicated that kaolin was mainly composed of silicon and aluminium with trace amounts of potassium.

The elemental-chemical analysis of ball clay by EDX showed presence of aluminium and silicon, thus confirming XRD results pointing to kaolin group. The EDX spectra also showed peaks of iron, potassium, calcium and titanium.

The observed feldspar peaks mainly contained metal cations such as sodium, calcium, aluminium and magnesium, and a large number of non-metallic elements such as silicon and oxygen. This kind of EDS spectra belongs to feldspar whose molecular formula is $(Na,Ca)AlSi_3O_8$. It was observed from table 4.6 that the spectrum had larger Na/Ca ratio than Ca/Na ratio indicating that the spectrum was for sodium feldspar whose name is sodium aluminium silicates and chemical formula of $NaAlSi_3O_8$ (Bühn & Rankin, 1999). The results indicated that sand was mainly composed of silica with trace amounts of aluminium oxide (Al_2O_3) and Iron (III) oxide (Fe_2O_3) as indicated in table 4.7.

5.2.4: **Modulus of Rapture (MOR) of Sample Tiles**

Tile sample A with composition ratio of 5:8:6:1 had the highest MOR followed by B with composition ratio 5:6:8:1, followed by C with composition ratio 5:5:9:1 and then D with composition ratio 5:4:10:1 had the least MOR. Tile sample with composition ratio of 5:8:6:1 had the highest mullite ($3Al_2O_3.2SiO_2$) content. Based on literature, the mechanical strength of ceramic ware depends on mullite ($3Al_2O_3.2SiO_2$) content and micro structure. The higher the mullite content, the higher the strength of the ceramic ware (Akwilapo & Wiik, 2004). The proportions of kaolin, feldspar, sand (quartz) and ball clay influence the phase compositions and mechanical properties of the fired ceramic tiles (Carty & Senapati, 2005). The high MOR of tile samples developed using composition ratio of 5:8:6:1 can be associated with the presence of mullite content and micro structure. Composition ratio of 5:8:6:1 had the highest kaolin content of 40%, whose chemical formula is identical to that of mullite compared to composition ratios of 5:6:8:1, 5:5:9:1 and 5:4:10:1 which had low kaolin content.

It was observed that the composition of kaolin and feldspar had an effect on MOR. As you reduce kaolin and increase feldspar while keeping ball clay and sand constant, there was a decrease in MOR. Therefore, according to this study, variation of kaolin and feldspar while keeping ball clay and sand fixed had an effect on the MOR. According to

the analysis made, tiles made using composition 5:8:6:1 had the highest mean value of MOR of 30.836 MPa compared to compositions 5:6:8:1, 5:5:9:1 and 5:4:10:1. A similar study was carried out by Ochen who developed porcelain floor tiles using raw materials found in Uganda and then tested their mechanical properties. He obtained a maximum strength of 34MPa which was in range with that of South African National standards (>34MPa) (Ochen, 2012). Therefore, composition A in the ratio of 5:8:6:1 was the recommended composition for production of tile samples.

5.2.5: Compressive Strength (CS) of Sample Tiles

Tile sample of composition ratio 5:8:6:1 had the highest MOR followed by 5:6:8:1, 5:5:9:1 and 5:4:10:1 which had the least MOR. It was observed that the composition of kaolin and feldspar had an effect on CS. As you reduced kaolin and increase feldspar while keeping ball clay and sand constant, there was a decrease in CS. Therefore, according to this study, variation of kaolin and feldspar while keeping ball clay and sand fixed had an effect on CS. According to the analysis made, tiles made using composition ratio of 5:8:6:1 had the highest mean value of CS of 1.358 MPa compared to compositions ratios of 5:6:8:1, 5:5:9:1 and 5:4:10:1. Another study carried out by Sultana et.al on mineralogical and physical characterization of clay used to produce tiles in Bangladesh indicated a maximum CS of 59MPa which was in range with ISSO standard value (between 53.38-59.8Pa)(Sultana et al., 2018). The big difference in the CS could be due to the difference in the chemical composition of the various clay deposits. Therefore, composition A in the ratio of 5:8:6:1 was the recommended composition for production of tile samples.

5.3: Conclusions

The production of ceramic floor tiles using ball clay, kaolin, feldspar and sand has been investigated in this present work. Ball clay was collected from Ntawo, kaolin from Buwambo, feldspar from Lunya and sand from Liddo beach in Wakiso. The raw materials were characterized by SEM, XRD, XRF and EDX before formulating the tiles. Mechanical properties i.e. MOR and CS of the developed tiles were tested.

The results for material characterization using SEM, XRD and EDX instruments have clearly shown that the experimental kaolin is a kaolinite mineral compound. The EDX results show the composition of Silicon and Aluminium in the experimental kaolin of 10.83 % and 11.15 % respectively. The results of the SEM and XRD analyses also

support the EDX results. From XRD diffractograms special peaks were obtained for kaolinite, feldspar, ball clay and sand. Results obtained confirmed that the feldspar used in this study is Sodium Aluminium Silicates **(**$NaAlSi_3O_8$) feldspar, EDX results for experimental ball clay matched with its XRD results thus confirming that the clay used was ball clay and the sand used was amorphous silica and hence lack any ordered crystalline structure.

Tile sample A with kaolin-feldspar ratio of 4:3 had the highest MOR of 30.836 MPa followed by B with kaolin-feldspar ratio of 3:4 followed by C with kaolin-feldspar ratio of 5:9 and D with kaolin-feldspar ratio of 2:5 had the least MOR of 18.58 MPa. It also had the highest CS of 1.358 MPa followed by B, C and D which had the least CS of 0.818MPa. In this study, the null hypothesis HO_2 was that the MOR of the tiles produced will not be affected by the composition ratios of the clay mixture. This was rejected at the two levels of significance of $\alpha = 0.01$ and $\alpha = 0.05$ since the MOR for the four compositions were statistically different at the two levels of significance. Similarly, the null hypothesis HO_1 that the CS of the tiles produced will not be affected by the composition ratios of the clay mixture was rejected at the two levels of significance of $\alpha = 0.01$ and $\alpha = 0.05$ since the CS for the four compositions were statistically different at the two levels of significance. It is observed that the composition of kaolin and feldspar has an effect on MOR and CS. As you reduce kaolin and increase feldspar while keeping ball clay and sand constant, there is a decrease in MOR and CS of the tile sample. Therefore, according to this study, variation of kaolin and feldspar while keeping ball clay and sand fixed has an effect on the MOR and CS of the tile sample.

The mechanical properties tested confirmed that the samples developed in this study using composition A with Buwambo kaolin-Lunya feldspar ratio of 4:3 and Ntawo ball clay-Liddo beach sand ratio of 5:1 possessed better mechanical properties of MOR and CS and therefore good for use as ceramic floor tiles compared to those developed using composition B, C and D.

5.4: Recommendations

The tile samples developed in this study using composition ratio 5:8:6:1 with Buwambo kaolin-Lunya feldspar ratio of 4:3 and Ntawo ball clay-Liddo beach sand ratio of 5:1 possessed better mechanical properties of modulus of rapture and compressive strength and therefore recommended for use in the manufacture of ceramic floor tiles.

Further investigation should be carried out;

The effect of alumina and silica quantities in kaolin and feldspar on modulus of rapture and compressive strength of ceramic tiles developed using kaolin, feldspar, ball clay and sand from other clay deposits.

REFERENCES

Abadir, M., Sallam, E., & Bakr, I. J. C. I. (2002). Preparation of porcelain tiles from Egyptian raw materials. *Ceramics International, 28*(3), 303-310.

Abdulabbas, A. A. (2022). Clay basics and their physical and chemical properties: Review Paper. *Innovative Infrastructure*

Acquafredda, P. J. P. S. R. (2019). XRF technique. *Physical Sciences Reviews, 4*(8).

Akwilapo, L. D., & Wiik, K. J. B. o. t. C. S. o. E. (2004). Ceramic properties of pugu kaolin clays. Part 2: Effect of phase composition on flexural strength. *Bulletin of the Chemical Society of Ethiopia, 18*(1).

Baioumy, H. M., & Ismael, I. S. J. A. C. S. (2014). Composition, origin and industrial suitability of the Aswan ball clays, Egypt. *Applied Clay Science, 102*, 202-212.

Bauluz, B. (2015). HALLOYSITE AND KAOLINITE: TWO CLAY MINERALS WITH GEOLOGICAL AND TECHNOLOGICAL IMPORTANCE. *Revista de la Real Academia de Ciencias. Zaragoza., 70*, 1-33.

Baynes, F., Fookes, P., Kennedy, J. J. B. o. E. G., & Environment, t. (2005). The total engineering geology approach applied to railways in the Pilbara, Western Australia. *Bulletin of Engineering Geology and the Environment, 64*, 67-94.

Beckett, R. G. (2020). XRF (X-Ray Fluorescence). In *Advances in Paleoimaging* (pp. 21-26): CRC Press.

Bergaya, F., & Lagaly, G. J. D. i. c. s. (2006). General introduction: clays, clay minerals, and clay science. *Developments in clay science, 1*, 1-18.

Bühn, B., & Rankin, A. J. G. e. C. A. (1999). Composition of natural, volatile-rich Na–Ca–REE− Sr carbonatitic fluids trapped in fluid inclusions. *Geochimica et Cosmochimica Acta,, 63*(22), 3781-3797.

Carty, W., & Senapati, U. (2005). Porcelain—Raw Materials, Processing, Phase Evolution, and Mechanical Behavior. *Journal of the American Ceramic Society, 81*, 3-20. doi:10.1111/j.1151-2916.1998.tb02290.x

Chauhan, A., & Chauhan, P. J. J. A. B. T. (2014). Powder XRD technique and its applications in science and technology. *J Anal Bioanal Tech, 5*(5), 1-5.

Dewi, R., Agusnar, H., & Alfian, Z. (2018). *Characterization of technical kaolin using XRF, SEM, XRD, FTIR and its potentials as industrial raw materials.* Paper presented at the Journal of Physics: Conference Series.

Dondi, M. (2007). *Mechanical and tribological properties of ceramic tiles: a reappraisal*: researchgate.net.

Elakhame, Z. U., Ifebhor, F., & Asotah, W. (2016). DEVELOPMENT AND PRODUCTION OF CERAMIC TILES FROM WASTE BOTTLE POWDER (MILLED GLASS). *Kathmandu University Journal of Science, Engineering and Technology, 12*, 50. doi:10.3126/kuset.v12i2.21521

Grim, R., & Kodama, H. (2021). Clay minerals. Encylopedia Britannica. In: Clay Clay Miner.

Grimshaw, R. W., & Searle, A. B. (1971). *The chemistry and physics of clays and allied ceramic materials*: Wiley-Interscience.

Halmurat, D., Yusufu, T., Wang, Q.-l., He, J., & Sidike, A. J. S. r. (2019). Rare earth ion Tb3+ doped natural sodium feldspar (NaAlSi3O8) Luminescent properties and energy transfer. *Scientific reports, 9*(1), 14637.

Islam, R. A. (2002). Study of structure-property relationship in high tension ceramic insulator. *Rashed Adnan Islam*.

Janssens, K., Vincze, L., Vekemans, B., Adams, F., Haller, M., & Knöchel, A. (1998). Use of Lead-glass Capillaries for Micro-focusing of Highly-energetic (0–60 keV) Synchrotron Radiation. *J. Anal. Atom. Spectrom., 13*, 339-350. doi:10.1039/A707700I

Joni, I. M., Nulhakim, L., Vanitha, M., & Panatarani, C. (2018). Characteristics of crystalline silica (SiO 2) particles prepared by simple solution method using sodium silicate (Na 2 SiO 3) precursor. *Journal of Physics: Conference Series, 1080*, 012006. doi:10.1088/1742-6596/1080/1/012006

Kanwal, F., Batool, D., Adnan, M., & Naseem, S. (2015). The effect of molecular structure, band gap energy and morphology on the dc electrical conductivity of polyaniline/aluminium oxide composites. *Materials Research Innovations, 19*, S8-354. doi:10.1179/1432891715Z.0000000001688

Kerr, P. F. (1952). Formation and Occurrence of Clay Minerals. *Clays and Clay Minerals, 1*(1), 19-32. doi:10.1346/CCMN.1952.0010104

Kingery, W. D., Bowen, H. K., & Uhlmann, D. R. (1976). *Introduction to ceramics* (Vol. 17): John wiley & sons.

Kirabira, J. B., Wijk, G., Jonsson, S., & Byaruhanga, J. K. J. s. r. i. (2006). Fireclay refractories from Ugandan kaolinitic minerals. *steel research international, 77*(8), 531-536.

Kumari, N., & Mohan, C. J. C. C. M. (2021). Basics of clay minerals and their characteristic properties. *Clay Clay Miner, 24*, 1-29.

Lal, R. (2006). *Encyclopedia of soil science*: CRC Press.

Lewicka, E., & Trenczek-Zajac, A. (2020). Investigations of Feldspar-Quartz Raw Materials After Firing: Effect of Various Na2O/K2O Ratio and Synthetic Pigments Addition. *Minerals, 10*(7), 646.

Luz, A., & Ribeiro, S. J. C. i. (2007). Use of glass waste as a raw material in porcelain stoneware tile mixtures. *Ceramics International, 33*(5), 761-765.

Moses, I. J., & Ben, E. J. I. J. I. S. R. T. (2018). The effect of holding time on the compressive strength o f Mukono Ntawo ball clay. *International Journal of Innovative Science and Research Technology, 3*, 281-288.

Murray, H. H. J. A. c. s. (1991). Overview—clay mineral applications. *Applied Clay Science, 5*(5-6), 379-395.

Nallathambi, G., Ramachandran, T., Venkatachalam, R., & Palanivelu, R. (2011). Effect of Silica Nanoparticles and BTCA on Physical Properties of Cotton Fabrics. *Materials Research, 14*, 552-559. doi:10.1590/S1516-14392011005000086

Nelson, S. A. J. T. U., Aug. (2015). Phyllosilicates (Micas, Chlorite, Talc, & Serpentine). *Tulane University, Aug, 18*.

Ochen, W. (2012). *Mechanical properties of ceramic floor tiles made from selected minerals in Uganda.* Kyambogo University.,

Odom, I., Fowden, L., Barrer, R., & Tinker, P. J. S. A., Math Phys Sci. (1984). clay minerals: properties and uses. *Philosophical transactions of the Royal Society of London, 311*, 391.

Olupot, P. W. (2010). *Characterization of Ceramic Raw Minerals in Uganda for Production of Electrical Porcelain Insulators*.

Olupot, P. W., Jonsson, S., & Byaruhanga, J. K. J. J. A. C. S. (2006). Characterization of feldspar and quartz raw materials in Uganda for manufacture of electrical porcelains. *J. Aust. Ceram. Soc, 42*(1), 29-35.

Pandey, A., Dalal, S., Dutta, S., & Dixit, A. J. J. o. M. S. M. i. E. (2021). Structural characterization of polycrystalline thin films by X-ray diffraction techniques. *Journal of Materials Science: Materials in Electronics, 32*(2), 1341-1368.

Pinet, S., Lartiges, B., Martinez, J.-M., & Ouillon, S. J. I. j. o. s. r. (2019). A SEM-based method to determine the mineralogical composition and the particle size distribution of suspended sediment.

International Journal of Sediment Research, 34(2), 85-94.

Powell, P. S. J. A. C. S. B. (1996). Ball clay basics. *American Ceramic Society Bulletin, 75*(6), 73-78.

Rahbar, N., Aduda, B. O., Zimba, J., Obwoya, S., Nyongesa, F., Yakub, I., & Soboyejo, W. J. E. m. (2011). Thermal shock resistance of a kyanite-based (aluminosilicate) ceramic. *Experimental Mechanics volume, 51*(2), 133-141.

Ryan, W. (1978). CHAPTER 5 - Ceramic Raw Materials. In W. Ryan (Ed.), *Properties of Ceramic Raw Materials (Second Edition)* (pp. 42-110): Pergamon.

Singer, F. (2013). *Industrial ceramics*: Springer.

Singer, F., & Singer, S. S. (1963). *Industrial ceramics*. London: Chapman & Hall.

Smallman, R. E., & Ngan, A. (2011). *Physical metallurgy and advanced materials*: Elsevier.

Stathis, G., Ekonomakou, A., Stournaras, C., & Ftikos, C. J. J. o. t. E. C. S. (2004). Effect of firing conditions, filler grain size and quartz content on bending strength and physical properties of sanitaryware porcelain. *Journal of the European Ceramic Society, 24*(8), 2357-2366.

Sultana, M. S., Zaman, M. N., Rahman, M. A., Biswas, P. K., Nandy, P. K. J. J. o. M., Characterization, M., & Engineering. (2018). Mineralogical and Physical Characterization of Clay of Sitakunda Anticline: Used for Ceramic Industries. *Journal of Minerals and Materials Characterization and Engineering, 6*(03), 333.

Takada, A., Richet, P., Catlow, C. R. A., & Price, G. D. (2004). Molecular dynamics simulations of vitreous silica structures. *Journal of Non-Crystalline Solids, 345-346*, 224-229. doi:https://doi.org/10.1016/j.jnoncrysol.2004.08.247

Ural, N. (2021). The significance of scanning electron microscopy (SEM) analysis on the microstructure of improved clay: An overview. *13*(1), 197-218. doi:doi:10.1515/geo-2020-0145

Wubet, W. (2019). Green Synthesis of CuO Nanoparticles for the Application of Dye Sensitized Solar Cell. *wjpr.s3.ap-south-1.amazonaws.com*.

Young, C. A. (2019). *SME mineral processing and extractive metallurgy handbook*: Society for Mining, Metallurgy & Exploration.

Zhang, Y., Hu, Y., Sun, N., Liu, R., Wang, Z., Wang, L., & Sun, W. (2018). Systematic review of feldspar beneficiation and its comprehensive application. *Minerals Engineering, 128*, 141-152. doi:https://doi.org/10.1016/j.mineng.2018.08.043

APPENDIX A

LIST OF RECENT STUDIES CARRIED ON UGANDAN CLAYS

Clay site	Characterization Method				Developed Tiles	Mechanical Properties of tiles made	Reference
	Chemical	Structural (XRD)	Morphology (SEM)	Thermal Analysis (TGA)			
- Mutaka (Bushenyi, Lunya (Kayunga) - Liddo beach(Wakiso)	-	✓	✓	✓	-	-	Olupot P.W 2010
Ntawo Mukono ball clay	XRD	-	-	-	-	-	(Moses & Ben, 2018)
- Mutaka kaolin rich clay - Mutundwe kaolin Mukono ball clay	✓	✓	✓	✓	-	-	(Kirabira et al., 2006)
- Mutaka - Ntawo -Liddo beach	XRF	-	-	-	✓	-Shrinkage -Strength -Water absorption	(Ochen, 2012)

APPENDIX B

RAW DATA FOR MODULUS OF RAPTUR AND COMPRESSIVE STRENGTH

Table 1: Modulus of Rapture of sample A

L/mm	b/mm	t/mm	t^2/mm^2	F/N	MOR/MPa
100.06	45.04	10.03	100.60	914.19	30.23
100.05	45.03	10.04	100.80	851.16	28.14
100.06	45.04	10.03	100.60	942.56	31.16
100.05	45.05	10.03	100.60	963.72	31.86
100.06	45.04	10.04	100.80	991.86	32.79

Table 2: Modulus of Rapture of sample B

L/mm	b/mm	t/mm	t^2/mm^2	F/N	MOR/MPa
100.35	45.70	10.70	114.49	809.54	26.76
100.36	45.69	10.72	114.92	817.67	27.03
100.37	45.71	10.71	114.70	833.95	27.57
100.35	45.69	10.71	114.70	890.47	29.44
100.36	45.68	10.70	114.49	850.00	28.10

Table 3: Modulus of Rapture of sample C

L/mm	b/mm	t/mm	t^2/mm^2	F/N	MOR/MPa
100.03	45.06	10.03	100.60	730.70	24.12
100.13	45.05	10.04	100.80	716.74	23.71
100.05	45.06	10.05	101.00	681.63	22.53
100.03	45.07	10.03	100.60	772.79	25.55
100.02	45.06	10.03	100.60	695.35	22.99

Table 4: Modulus of Rapture of sample D

L/mm	b/mm	t/mm	t^2/mm^2	F/N	MOR/MPa
100.02	45.03	10.02	100.40	546.51	18.10
100.00	45.04	10.00	100.00	560.70	18.54
100.02	45.03	10.03	100.60	567.44	18.76
100.03	45.05	10.02	100.40	574.65	18.99
100.02	45.03	10.00	100.00	560.70	18.54

Table 5: Compressive Strength for sample A

L/mm	b/mm	t/mm	A/mm^2	F /kN	CS/MPa
107.06	45.04	10.04	4821.98	6.60	1.37
107.04	45.03	10.03	4820.01	6.25	1.29
107.06	45.05	10.03	4823.05	6.45	1.34
107.05	45.04	10.04	4821.53	6.75	1.40
107.06	45.04	10.05	4821.98	6.65	1.38

Table 6: Compressive Strength for sample B

L/mm	b/mm	t/mm	A/mm^2	F /kN	CS/MPa
109.36	45.69	12.71	4996.66	5.20	1.04
109.35	45.70	12.70	4997.30	5.35	1.07
109.36	45.68	12.72	4995.56	5.45	1.09
109.34	45.69	12.71	4995.74	5.50	1.10
109.36	45.70	12.71	4997.75	5.35	1.07

Table 7: Compressive Strength for sample C

L/mm	b/mm	t/mm	A/mm^2	F /kN	CS/MPa
110.03	46.06	12.03	5067.98	5.25	1.04
109.36	46.05	12.04	5036.03	5.15	1.02
109.36	46.06	12.03	5037.12	5.05	0.99
109.35	46.07	12.02	5037.75	5.35	1.10
109.37	46.06	12.03	5037.58	5.00	0.99

Table 8: Compressive Strength for sample D

L/mm	b/mm	t/mm	A/mm^2	F /kN	CS/MPa
107.02	45.03	11.02	4819.11	3.85	0.80
107.01	45.04	11.01	4819.73	4.05	0.84
107.02	45.03	11.02	4819.11	3.85	0.80
107.03	45.02	11.03	4818.49	3.95	0.82
107.02	45.03	11.02	4819.11	4.00	0.83

APPENDIX C

TABLES OF DATA USED FOR DETERMINATION OF PARTICLE SIZE

Table 9: Particle size distribution of SEM image for feldspar

Number	Area /µm
1	0.11
2	0.522
3	0.089
4	0.028
5	0.156
6	0.067
7	0.207
8	0.118
9	0.191
10	0.048
11	0.069
12	0.094
13	0.086
14	0.107
15	0.418
16	0.087
17	0.334
18	0.159
19	0.173
20	0.194
21	0.283
22	0.227
23	0.165
24	0.153
25	0.268
26	0.409

27	0.268
28	0.06
29	0.119
30	0.126
31	0.176
32	0.131
33	0.11
34	0.144
35	0.311
36	0.111
37	0.113
38	0.184
39	0.068
40	0.186
41	0.062
42	0.06
43	0.039
44	0.04
45	0.134
46	0.15
47	0.094
48	0.071
49	0.091
50	0.062
Mean	0.153
SD	0.105
Min	0.028
Max	0.522

Table 10: Particle size distribution of SEM image for kaolin

Number	Area / µm
1	0.433
2	0.332
3	0.15
4	0.157
5	0.08
6	0.274
7	0.089
8	0.451
9	0.146
10	0.106
11	0.438
12	0.223
13	0.031
14	0.186
15	0.164
16	0.319
17	0.477
18	0.066
19	0.065
20	0.097
21	0.237
22	0.082
23	0.222
24	0.114
25	0.217
26	0.385
27	0.082
28	0.072
29	0.199
30	0.167

Mean	0.202
SD	0.131
Min	0.031
Max	0.477

Table 11: Particle size distribution of SEM image for ball clay

Number	Area / µm
1	0.185
2	0.057
3	0.033
4	0.036
5	0.109
6	0.137
7	0.083
8	0.093
9	0.088
10	0.068
11	0.172
12	0.053
13	0.139
14	0.096
15	0.059
16	0.064
17	0.05
18	0.118
19	0.095
20	0.119
21	0.061
22	0.083
23	0.047
24	0.129
25	0.079
26	0.081
27	0.086
28	0.038
29	0.154
30	0.219
31	0.063
32	0.05

33	0.076
34	0.097
35	0.033
36	0.05
37	0.035
38	0.08
39	0.128
40	0.067
41	0.063
42	0.288
43	0.028
44	0.044
45	0.193
46	0.052
47	0.163
48	0.113
49	0.191
50	0.083
Mean	0.095
SD	0.055
Min	0.028
Max	0.288

Table 12: Particle size distribution of SEM image for sand

Number	Area / µm
1	0.054
2	0.023
3	0.014
4	0.017
5	0.049
6	0.233
7	0.1
8	0.228
9	0.031
10	0.281
11	0.059

12	0.186
13	0.081
14	0.037
15	0.192
16	0.235
17	0.02
18	0.021
19	0.217
20	0.059
21	0.214
22	0.715
23	0.249
24	0.235
25	0.293
26	0.262
27	0.244
28	0.21
29	0.287
30	0.144
31	0.048
32	0.691
33	0.155
34	0.838
35	0.04
36	0.101
37	0.046
38	0.045
39	0.047
40	0.097
41	0.788
42	0.024
43	0.084

44	0.03
45	0.062
46	0.032
47	0.124
48	0.053
49	0.062
50	0.021
Mean	0.168
SD	0.198
Min	0.014
Max	0.838

APPENDIX D

PERCENTAGE OF ELEMENTAL DISTRIBUTION IN RAW MATERIALS

Table 13: Percentage of elemental distribution of all elements present in kaolin

Weight (%)							Ratio		
Spectrum	C	O	Al	Si	K	Total	Si/Al	Si/O	Al/O
Spectrum 1	28.43	54.23	8.57	8.3	0.47	100	0.97	0.21	0.22
Spectrum 2	30.46	49.59	9.87	9.47	0.61	100			
Spectrum 3	32.43	42.88	12.85	11.84	0	100			
Spectrum 4	9.93	60.52	14.13	14.64	0.78	100			
Spectrum 5	28.66	50.83	10.33	9.91	0.27	100			
Mean	25.98	51.61	11.15	10.83	0.43	100			
Std. deviation	9.12	6.46	2.28	2.48	0.3				
Max	32.43	60.52	14.13	14.64	0.78				
Min	9.93	42.88	8.57	8.3	0				

Table 14: Percentage of elements present in Ball clay

Weight (%)										
Spectrum	C	O	Na	Al	Si	K	Ca	Ti	Fe	Total
Spectrum 1	27.83	46.07	0.67	7.18	14.58	0.5	0.9	0.54	1.73	100
Spectrum 2	40.12	45.88	0.29	3.35	9.23	0.19	0.15	0.16	0.63	100
Spectrum 3	35.45	48.77	0.49	5.31	8.44	0.17	0.27	0.26	0.83	100
Spectrum 4	44.57	39.87	0.31	4.81	7.94	0.56	0.46	0.4	1.1	100
Spectrum 5	26.03	47.07	0.19	1.93	24.38	0	0.26	0.14	0	100
Mean	34.8	45.53	0.39	4.52	12.91	0.28	0.41	0.3	0.86	100
Std. deviation	7.9	3.37	0.19	1.99	6.94	0.24	0.3	0.17	0.63	
Max.	44.57	48.77	0.67	7.18	24.38	0.56	0.9	0.54	1.73	
Min.	26.03	39.87	0.19	1.93	7.94	0	0.15	0.14	0	

Table 15: Percentage of elements present in feldspar

Weight (%)									Ratios	
Spectrum	C	O	Na	Mg	Al	Si	Ca	Total	Ca/Na	Na/Ca
Spectrum 1	24.57	47.03	5.36	0.49	0.29	18.48	3.78	100	0.71	1.40
Spectrum 2	23.71	49.75	5.01	0.57	0.38	17.92	2.67	100		
Spectrum 3	12.62	53.49	7.05	0.8	0.62	22.15	3.28	100		
Spectrum 4	23.86	49.03	4.00	0.54	0.4	16.08	6.08	100		
Spectrum 5	16.10	50.46	5.90	0.33	0.54	23.04	3.64	100		
Mean	20.17	49.95	5.46	0.55	0.44	19.53	3.89	100		
Std. deviation	5.46	2.36	1.12	0.17	0.13	2.95	1.3			
Max.	24.57	53.49	7.05	0.8	0.62	23.04	6.08			
Min.	12.62	47.03	4	0.33	0.29	16.08	2.67			

APPENDIX E

STATISTICAL DATA FOR MODULUS OF RAPTURE AND COMPRESSIVE STRENGTH

Table 16: Statistical data obtained for Modulus of Rapture for the Tile samples.

	Modulus of Rapture/MPa							
Mixture ratios	**A (**5:8:6:1)		**B (**5:6:8:1)		**C (**5:5:9:1)		**D (**5:4:10:1)	
Mean $\bar{X}$	$\bar{X} =$ 30.836	$\bar{X}^2 =$ 953.380	$\bar{X} =$ 27.780	$\bar{X}^2 =$ 772.629	$\bar{X} =$ 23.788	$\bar{X}^2 =$ 566.963	$\bar{X} =$ 18.580	$\bar{X}^2 =$ 345.309
S.D (δ)	δ = 1.775		δ =1.061		$\delta =$ 1.169		$\delta =$ 0.341	
Max Error α=0.01	2.672		1.597		1.760		0.512	
Max Error α=0.05	1.599		0.956		1.054		0.307	

Table 17: Statistical data obtained for compressive strength for the tile samples (five measurements of each sample).

	Compressive Strength /MPa							
Mixture ratios	**A (**5:8:6:1)		**B (**5:6:8:1)		**C (**5:5:9:1)		**D (**5:4:10:1)	
Mean $\bar{x}$	$\bar{X} =$ 1.358	$\bar{X}^2 =$ 1.358	$\bar{X} =$ 1.074	$\bar{X}^2 =$ 1.1539	$\bar{X} =$ 1.018	$\bar{X}^2 =$ 1.03722	$\bar{X} =$ 0.818	$\bar{X}^2 =$ 0.66938
S.D (δ)	$\delta =$ 0.038987		$\delta =$ 0.02302		$\delta =$ 0.033466		$\delta =$ 0.017889	
Max Era α=0.01	0.058673		0.034646		0.050364		0.026921	
Max Era α=0.05	0.035134		0.020746		0.030159		0.01612	